Hydrogen Separation from Gas Mixtures by Selective Adsorption

A/Prof Gang Kevin Li

Table of Contents

Outline

Background

Strength of hydrogen energy:

- ✓ Great flexibility storage and handling capacities.
- ✓ Stored in large quantities for extended periods of time.
- ✓ Obtained from different sources and different processes.

Application of hydrogen energy:

- ✓ As transport fuel for light vehicles and heavy vehicles.
- ✓ Stationary applications, for instance energy autonomy for buildings.
- ✓ Integration in centralized energy networks.

Hydrogen is proposed as an attractive substance that could be used to store and transport energy.

1. Martin, A., Agnoletti, M. F., & Brangier, E. (2020). Users in the design of Hydrogen Energy Systems: A systematic review. *International Journal of Hydrogen Energy*, *45*(21), 11889-11900.
2. Ibeh, B., Gardner, C., & Ternan, M. (2007). Separation of hydrogen from a hydrogen/methane mixture using a PEM fuel cell. *International journal of hydrogen energy*, *32*(7), 908-914.

Introduction

Hydrogen could be transported to various costumers via

- Gaseous hydrogen
  - ❑ Gaseous compression
  - ❑ **Pipelines**
  - ❑ Tube trailers
- Liquid hydrogen
- Novel hydrogen carriers
- Dispensing hydrogen fuel to vehicles
- Solid state storage

- Pipelines are the most efficient for handling large flows, but capital intensive ($0.5-$1.5 million/mile).
- The most cost efficient way is using the existing natural gas grid infrastructure.

Introduction

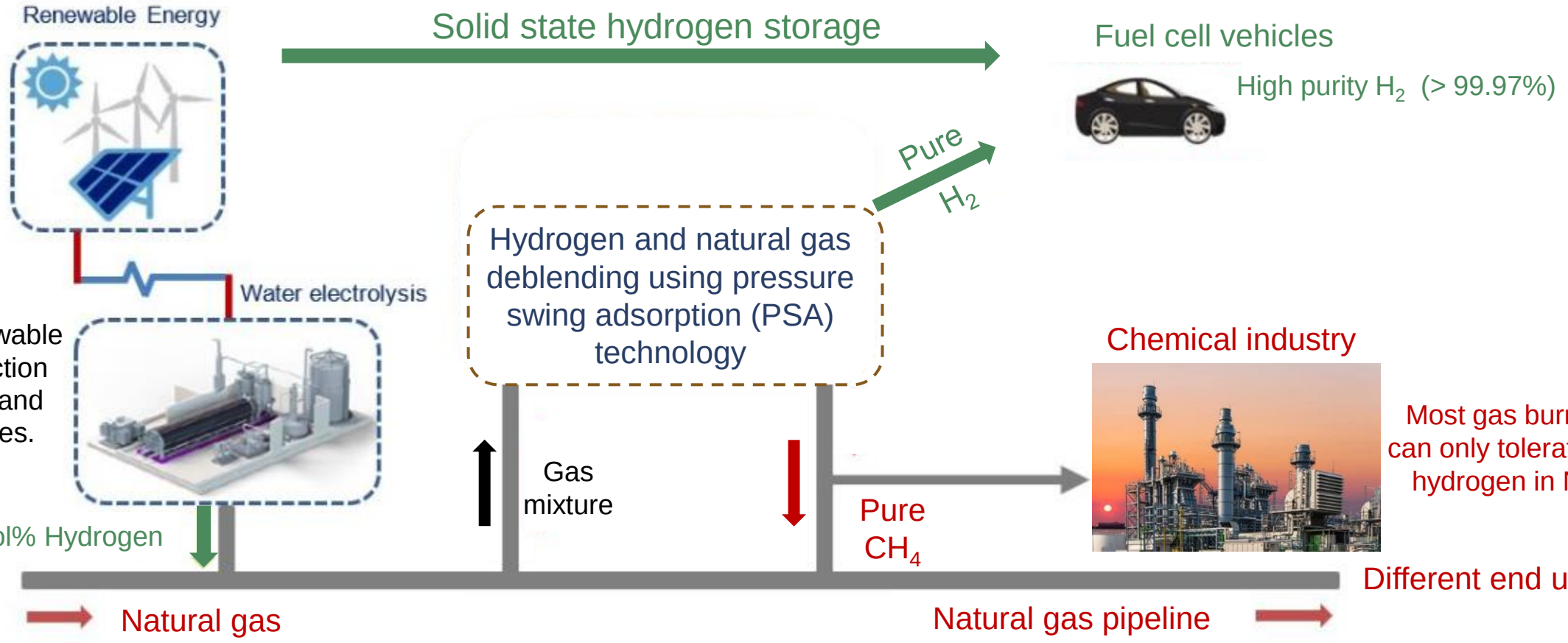

Hydrogen Park South Australia (HyP SA)

- The project facilities became operational on 19 May 2021.
- The renewable hydrogen is blended with natural gas at volumes of up to 10%, and supplied to nearby homes via the existing gas network.
- HyP SA is Australia's largest electrolyser and the first to deliver a renewable hydrogen blend to customers on the existing gas network.

Fast facts	
Online	May 2021
Electrolyser	1.25MW Proton Exchange Membrane (PEM)
Production	Up to 20kg per hour
Storage	40kg onsite
Electricity	Renewable electricity via grid*
Water	15L of ultrapure water for 1kg of hydrogen**
Markets	Up to 10% (volume) renewable gas blend to more than 3700 connections, businesses and schools and 100% to industry via tube trailers

* AGN will purchase (and voluntarily surrender) Large Scale Generation Certificates as required to ensure the electricity used to produce hydrogen is renewable.

** For context, in South Australia, the average person uses 190L of water per day. Running the HyP SA facility for 1 hour is the equivalent of a 30 minute shower with a low flow showerhead.

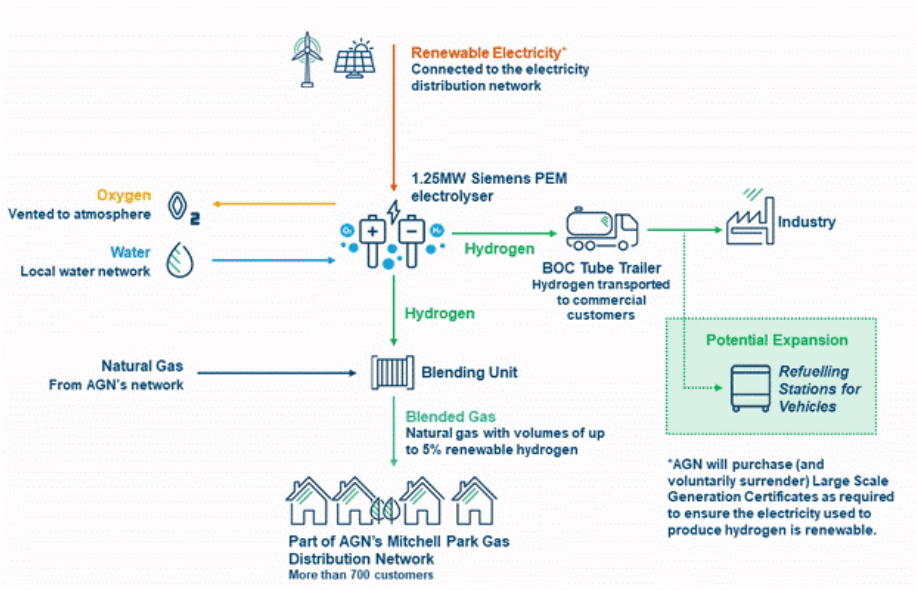

Australian Gas Infrastructure Group. (2022). *Australia's first renewable gas blend supplied to existing customers*. https://www.agig.com.au/hydrogen-park-south-australia

Hydrogen blending projects

Project name	Project period	Location	H_2% blending
HyNTS future grid	2019- present	UK	2
ITM Power Thüga Frankfurt plant	2014- present	Germany	2
The P2G-unit of the Bavarian city of Haßfurt	2016- present	Germany	5
Hydrogen Park South Australia	2019- present	Australia	5
GRTgaz Jupiter 1000 project	2017- present	France	0-6
HyDeploy	2019- present	UK	20
The GRHYD demonstration project	2014- present	France	0-20

ITM Power Thüga Frankfurt plant in Germany

GRTgaz Jupiter 1000 project in France

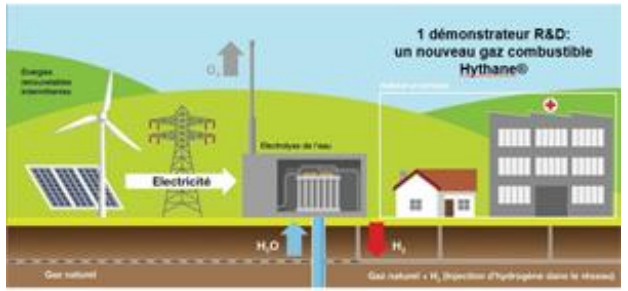

The GRHYD demonstrator makes it possible to valorize the ENR (green electricity not finding an outlet on the electricity network) in the form of hydrogen gas distributed in the natural gas network, by implementing the Power-to-Gas concept.

Raju, A. S. K., & Martinez-Morales, A. (2022). *Hydrogen Blending Impacts Study*. The California Public Utilities Commission. https://docs.cpuc.ca.gov/PublishedDocs/Efile/G000/M493/K760/493760600.PDF

Research challenges and gaps

- Minor component H_2 is the favored component to be captured.
- The hydrogen molecule is one of the smallest size molecule that exists.
- Traditional adsorbents (such as activated carbon, zeolite 5A and silica) have a higher capacity of CH_4 molecules.

Traditional adsorbent adsorbs CH_4 preferentially.

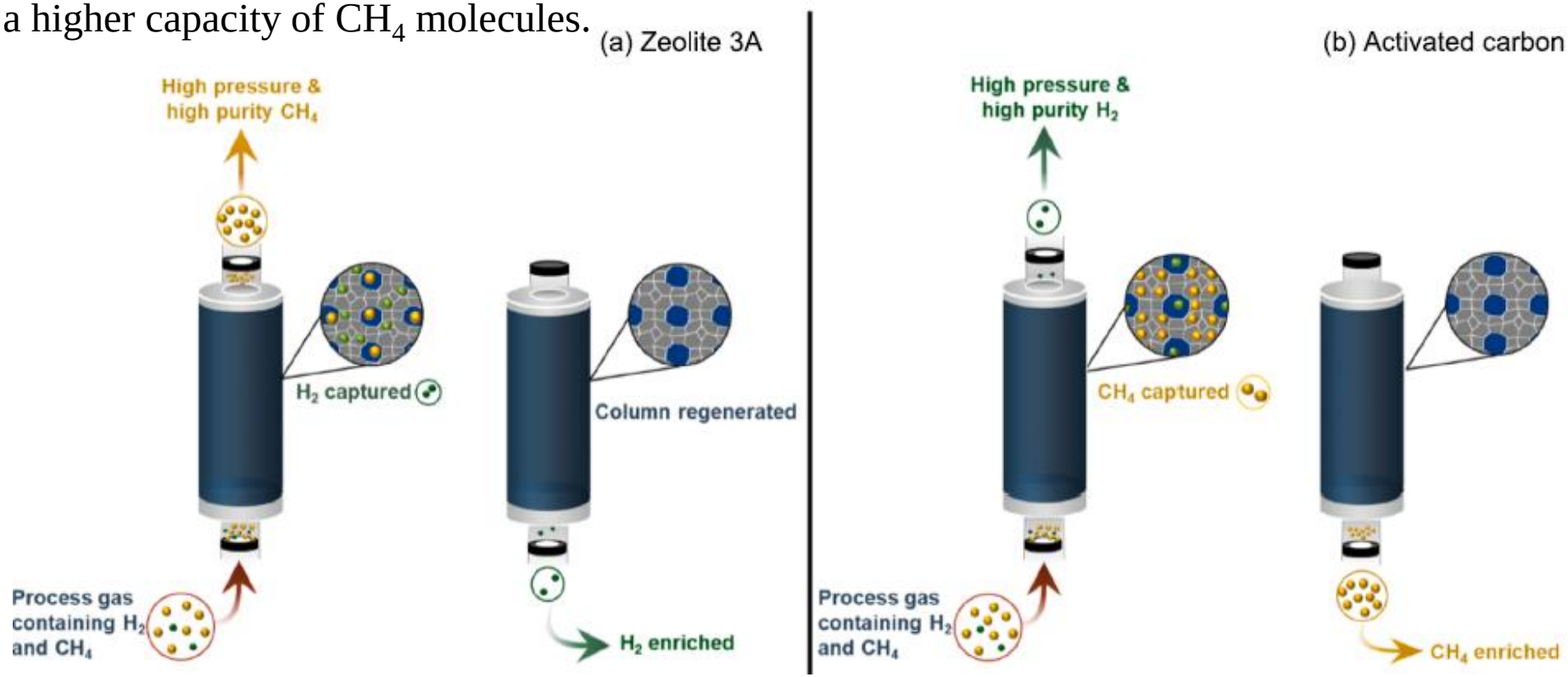

Adsorption and desorption process configuration using H_2 selective material - zeolite 3A (a) and CH_4 selective material - activated carbon (b).

Our innovations

1 - Hydrogen capture using zeolite 3A for pipeline gas deblending

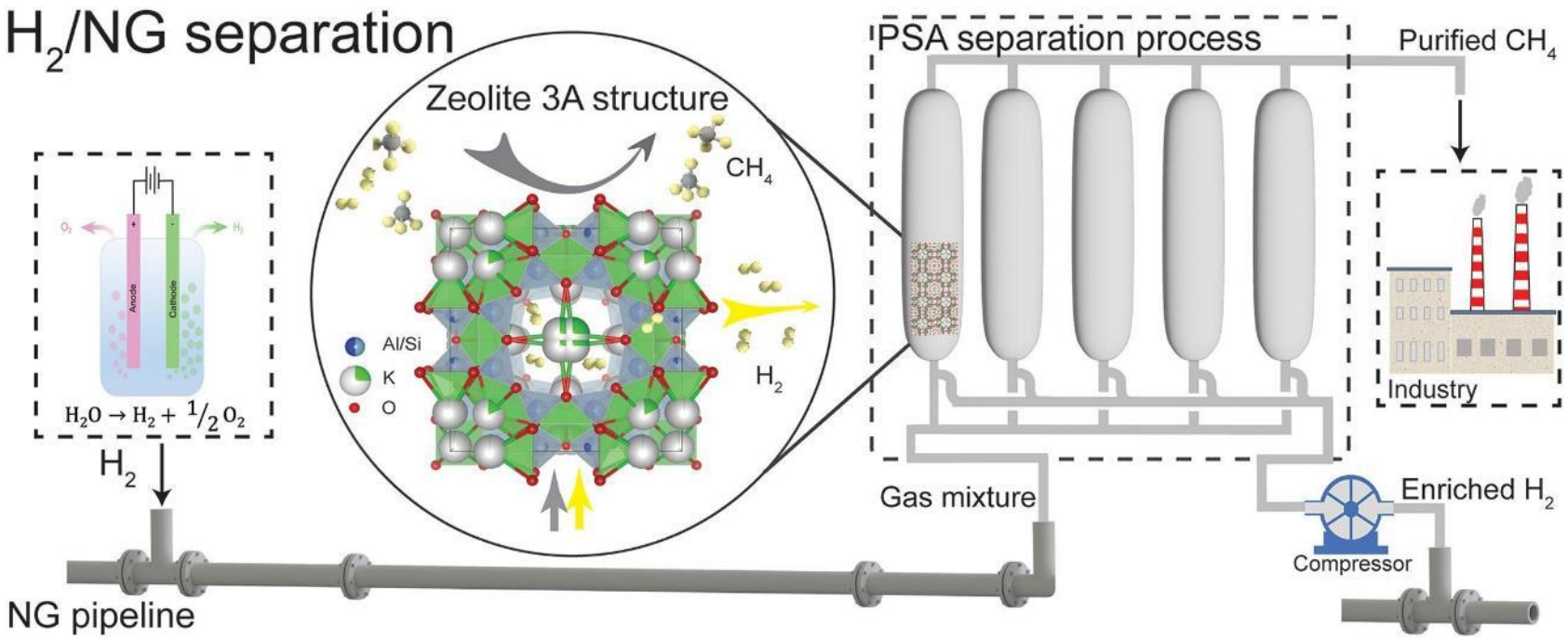

Zeolite 3A

Properties:

- The chemical formula is $K_{12}[(AlO_2)_{12}(SiO_2)]\cdot XH_2O$.
- Zeolite 3A has the molecular-sieving windows of nominal diameter 0.3 nm (3Å) in its crystal lattice framework, which obstruct the adsorption of molecules of diameter larger than 0.3 nm.

Applications:

- Hydrogen–deuterium isotope separation at low temperature (below 100 K).
- Dewatering (such as ethanol Dehydration - to obtain higher quality alcohol)

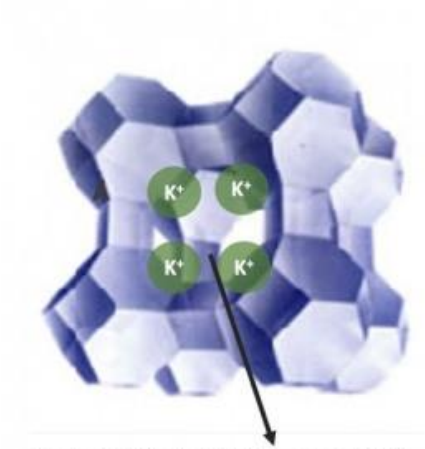

Molecular Sieve 3A: Pore diameter 3Å

Gas molecule	Kinetic diameter (Å)
H_2O	2.65
H_2	2.89
CO_2	3.3
O_2	3.46
N_2	3.64
CH_4	3.8

1. Salazar, J. M., Lectez, S., Gauvin, C., Macaud, M., Bellat, J. P., Weber, G., ... & Simon, J. M. (2017). Adsorption of hydrogen isotopes in the zeolite NaX: Experiments and simulations. *International Journal of Hydrogen Energy*, *42*(18), 13099-13110.
2. Kotoh, K., Takashima, S., & Nakamura, Y. (2009). Molecular-sieving effect of zeolite 3A on adsorption of H2, HD and D2. *Fusion engineering and design*, *84*(7-11), 1108-1112.
3. Pechar, T. W. (2004). *Fabrication and characterization of polyimide-based mixed matrix membranes for gas separations* (Doctoral dissertation, Virginia Tech).

Adsorbent selection

- ASAP Analyzer for ad

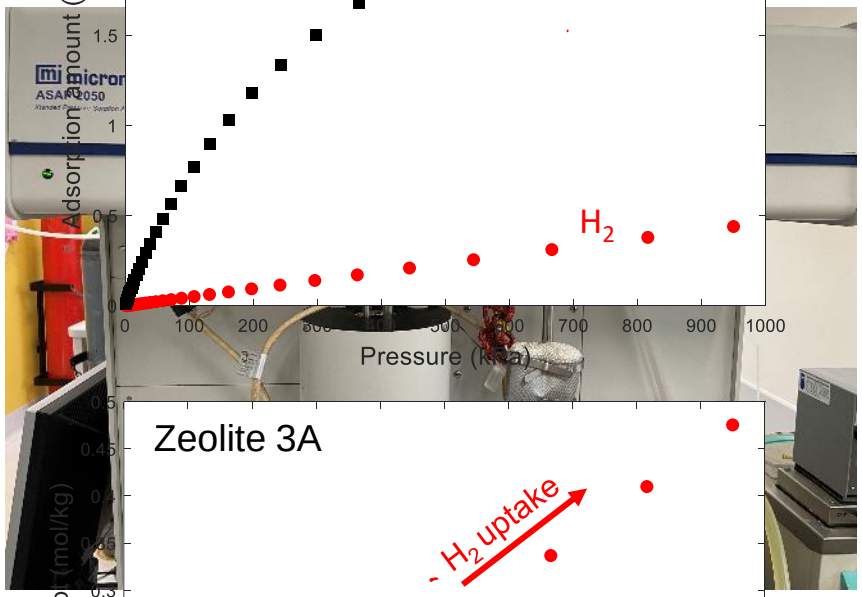

Resolu ucer)

Pressure: 10 bar	Zeolite 3A (25°C, 40°C and 60°C)	Zeolite 4A (25°C)
CH_4 adsorption	No adsorption	2.534 mmol/g

- The adsorption amount of both **CH_4** and **N_2** on zeolite 3A was too small for reliable measurement using ASAP 2050.

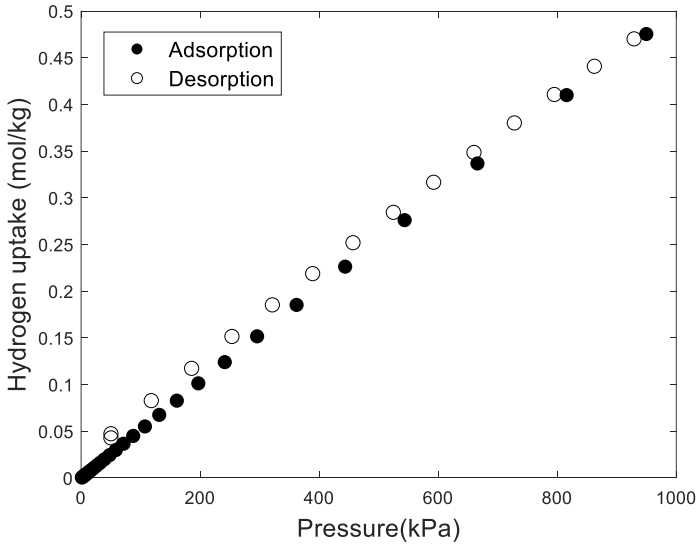

Could be a good choice for cyclic adsorption process!

Adsorption and desorption isotherms of H_2 on zeolite 3A at 298 K.

Materials characterization

- SEM and TEM images both revealed the cubic morphology of the zeolite 3A.
- XRD pattern confirmed the cubic crystal structure $K_{12}Al_{12}Si_{12}O_{48}$ with space group Pm3m.

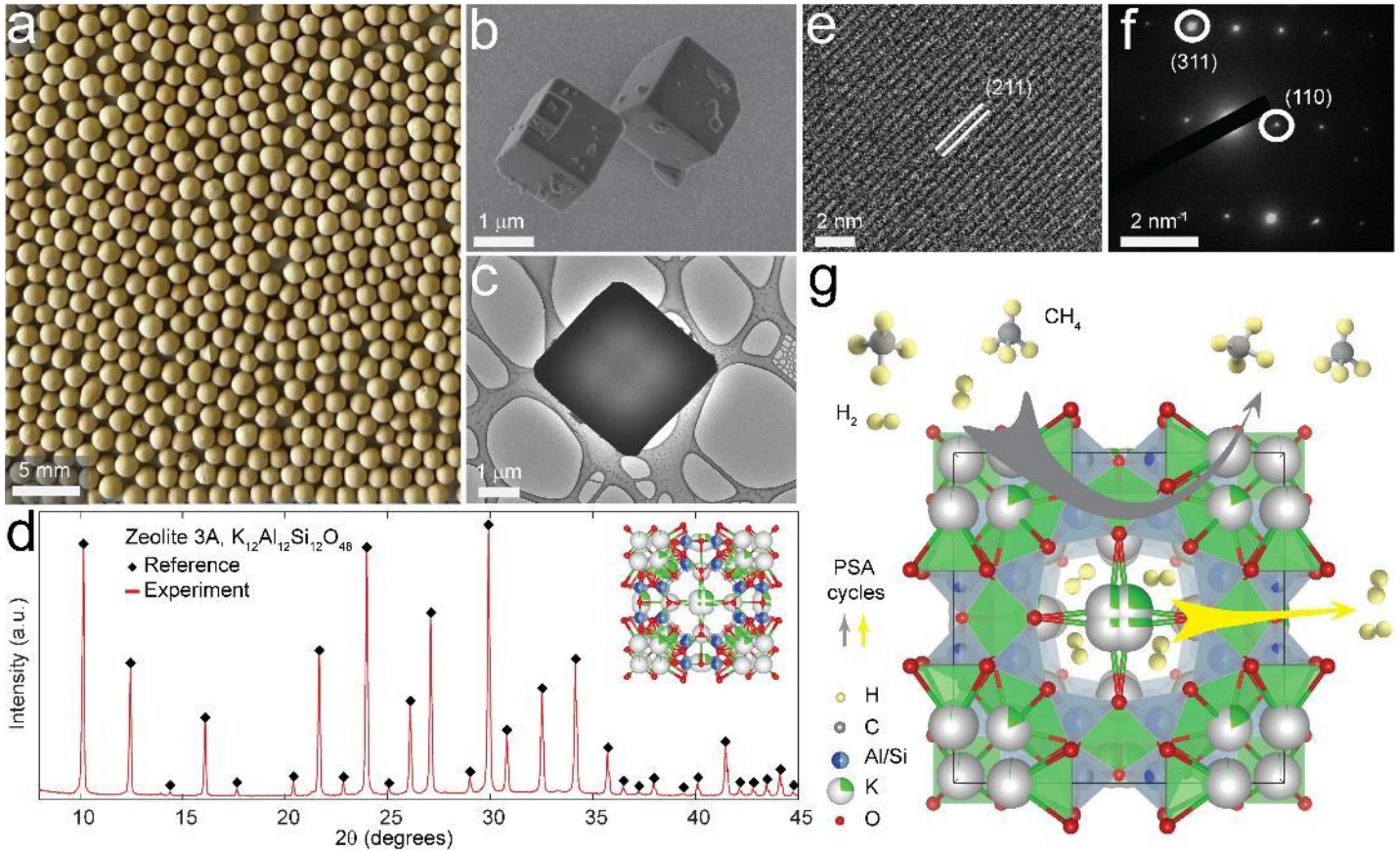

Characterization of adsorption materials zeolite 3A. optical image of zeolite beads (a), SEM micrographs of the zeolite cubes (b), TEM image confirming cube morphology of the zeolite (c), XRD pattern (d), HRTEM image of the zeolite 3A showing lattice fringes (e), TEM Selected Area Electron Diffraction (SAED) micrograph of zeolite featuring indexed reflections (f) and aperture of zeolite 3A and hydrogen selectivity configuration (g).

Hydrogen adsorption on zeolite 3A

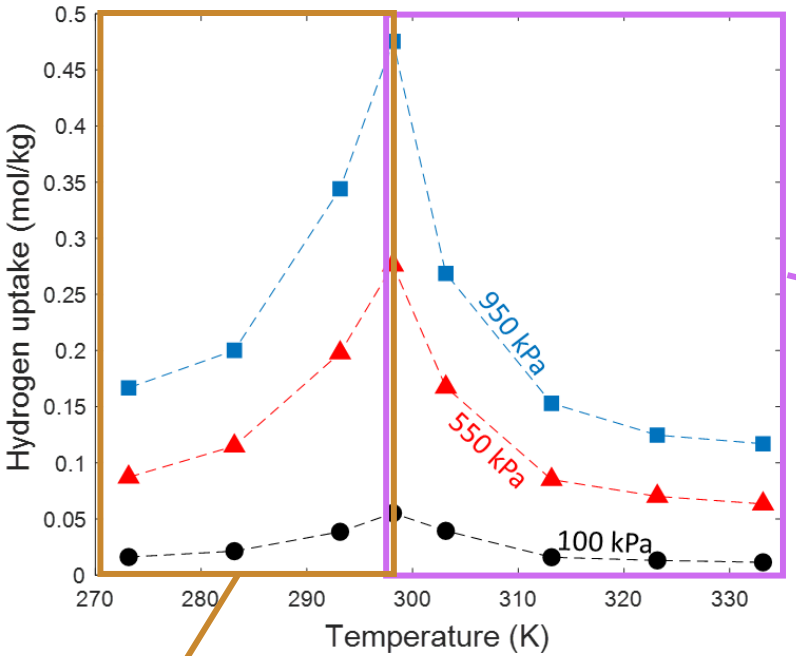

Hydrogen adsorption isobars (showing a peak at a near room temperature of 298 K).

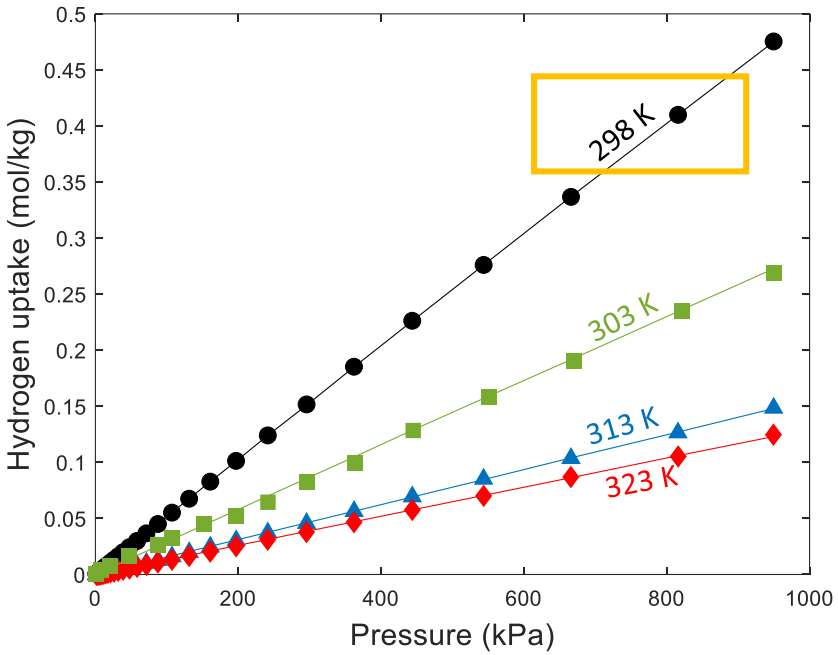

Adsorption isotherms of H_2 on zeolite 3A at different temperatures over the pressure range 0 to 1000 kPa, lines = Dual-site Langmuir model and symbols = experimental data.

Molecular trapdoor effect:

- The accessibility of adsorption sites is temperature dependent.
- H_2 gas can be adsorbed above a certain temperature.

Dual-site Langmuir model:

$$q_i^* = m_i \frac{b_i P_i}{1 + \sum_{j=1}^{N} b_j P_j} + n_i \frac{d_i P_i}{1 + \sum_{j=1}^{N} d_j P_j}$$

$$b_i = b_{i0} \exp\left(\frac{Q_{1,i}}{RT}\right) \quad d_i = d_{i0} \exp\left(\frac{Q_{2,i}}{RT}\right)$$

1. Li, G. K., Shang, J., Gu, Q., Awati, R. V., Jensen, N., Grant, A., ... & May, E. F. (2017). Temperature-regulated guest admission and release in microporous materials. *Nature communications*, *8*(1), 1-9.
2. Shang, J., Li, G., Singh, R., Gu, Q., Nairn, K. M., Bastow, T. J., ... & Webley, P. A. (2012). Discriminative separation of gases by a "molecular trapdoor" mechanism in chabazite zeolites. *Journal of the American Chemical Society*, *134*(46), 19246-19253.

Separation target and conditions

- Most of the currently installed gas turbines were specified for a H_2 fraction in natural gas of 1 vol% or even lower.

		[%]→	2	5	10	20	25	30	40	50	60	70	80	90	100
TS	Pipeline (steel, > 16 bar)	10%													
TS	Compressors	5%													
ST	Storage (cavern)	100%													
ST	Storage (porous)														
ST	Dryer	5%													
TS/DS	Valves	10%													
TS/DS	Process gas chromatographs														
TS/DS	Volume converters	10%													
TS/DS	Volume measurement	10%													
DS	Pipeline (plastics, < 16 bar)	100%													
DS	Pipeline (steel, < 16 bar)	25%													
DS	House installation	30%													
U	Gas engines	10%													
U	Gas cooker	10%													
U	Atmospheric gas burner	10%													
U	Condensing boiler	10%													
U	CNG-vehicles	2%													
U	Gas turbines	1%													
U	Feedstock														

Limitations for H_2 blending rates of selected components of gas utilization options.
Note: without adjustments (dark green), modifications may be needed (light green)

- New South Wales (Australia) pipeline network configuration

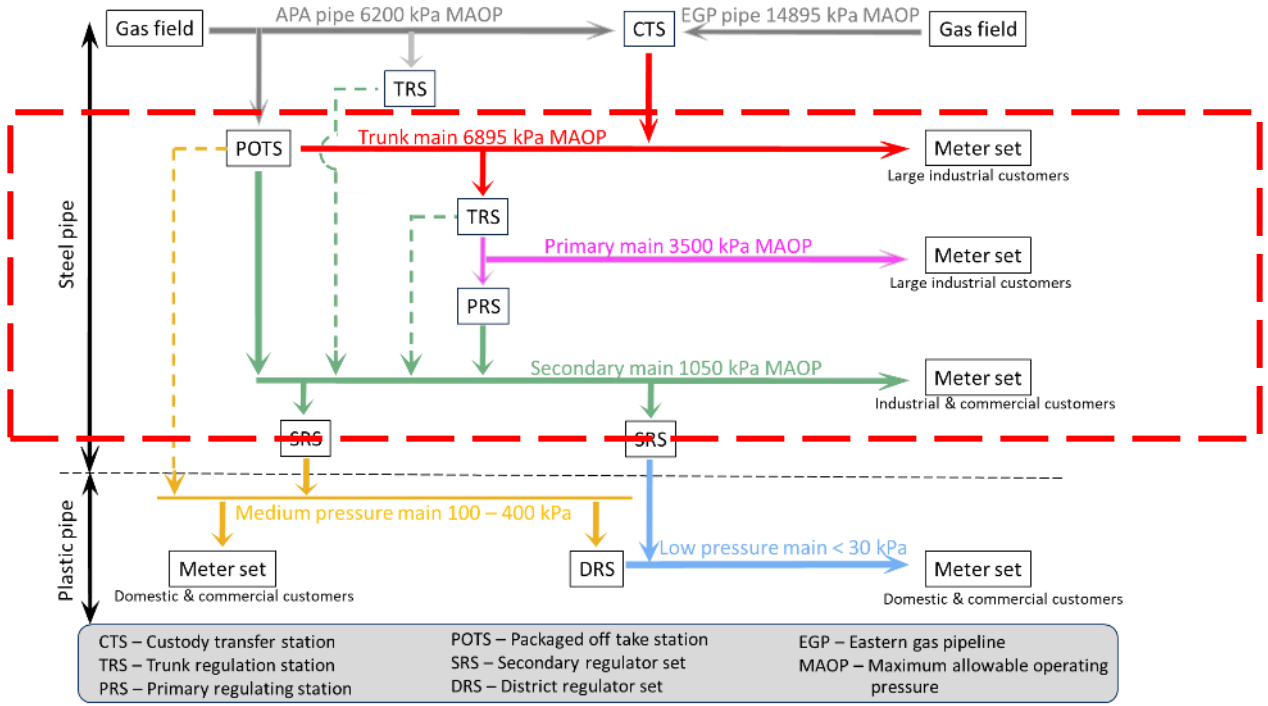

- Methane product purity > 99%
- Inlet pressures to be investigated: 10 bar, 30 bar, 50 bar

1. Bard, J., Gerhardt, N., Selzam, P., Beil, M., Wiemer, M., & Buddensiek, M. (2022). The Limitations of Hydrogen Blending in the European Gas Grid.
2. Altfeld, K., & Pinchbeck, D. (2013). Admissible hydrogen concentrations in natural gas systems. Gas Energy, 2103(03), 1-2
3. Smith, N., Byrne, N., Coates, M., Linton, V., & van Alphen, K. (2017). Research Report Identifying the commercial, technical and regulatory issues for injecting renewable gas in Australian distribution gas networks
4. Detailed Design for Hydrogen Generation (Western Sydney Green Gas Project), GPA Engineering, Australia, 2020

Separation performance_10 bar VPSA

- Step configuration: 5-bed VPSA process, 10 steps each cycle

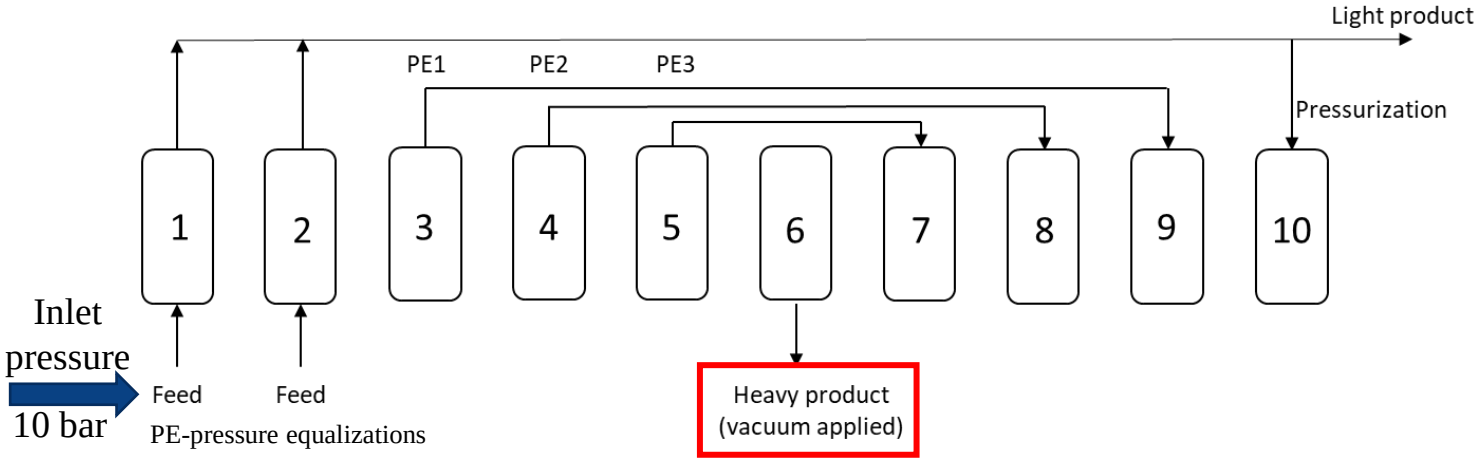

Simulation conditions

Condition	Value	Unit
Feed pressure	10	bar
Feed gas H_2 concentration	3, 4, 5, 10, 15	%
Desorption pressure	0.2	bar
Flow rate	100	sm^3/h
Operating temperature	298	K
Bed porosity	0.37	/

Physical size (m)	Feed H_2 concentration (%)	H_2 downstream concentration (%)	CH_4 topstream concentration (%)	H_2 recovery rate (%)	CH_4 recovery rate (%)	Energy consumption (kJ/kg CH_4)
0.5 x 1.8	3	7.76	99.01	76.75	71.78	70.63
	4	9.27	99.03	84.53	65.54	87.08
	5	11.10	99.04	88.42	62.74	128.91
	10	17.66	98.98	95.33	50.62	222.08
	15	22.59	99.10	97.91	40.80	377.62

Effect of vacuum level

Separation performance of 10 bar VPSA for various vacuum levels

Desorption pressure (kPa)	Feed H_2 concentration (%)	Cycle time (s)	H_2 downstream concentration (%)	CH_4 topstream concentration (%)	H_2 recovery rate (%)	CH_4 recovery rate (%)	Energy consumption (kJ/kg CH_4)
10	3	560	8.20	99.00	76.06	73.67	97.50
	4	470	9.82	99.00	83.51	68.03	126.25
	5	410	11.50	99.02	87.96	64.38	167.50
	10	275	17.89	99.03	95.46	51.31	333.13
	15	250	23.33	99.05	97.66	43.36	541.25
20	3	550	7.76	99.01	76.75	71.78	70.63
	4	435	9.27	99.03	84.53	65.54	86.88
	5	395	11.10	99.04	88.42	62.74	128.75
	10	270	17.32	99.07	95.88	49.15	250.00
	15	240	22.64	99.00	97.67	41.10	340.63
30	3	480	7.44	99.03	77.73	70.07	52.50
	4	410	9.07	99.05	85.23	64.40	75.63
	5	365	10.58	99.06	89.11	60.35	96.25
	10	250	16.60	99.07	96.11	46.35	171.88
	15	240	22.51	99.01	97.58	40.74	275.63

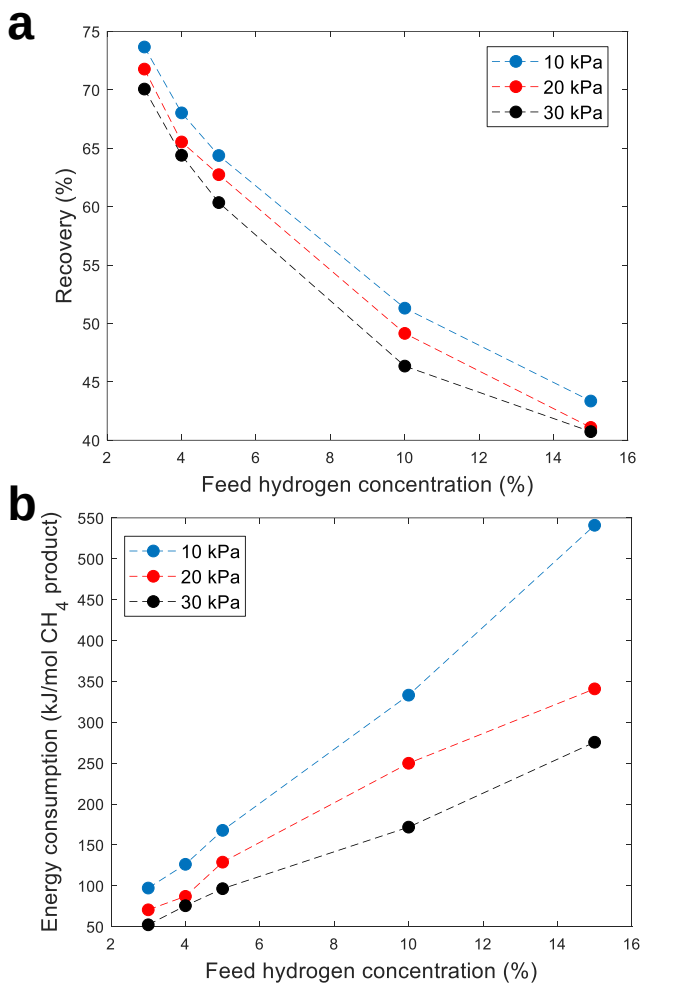

CH_4 product recovery (a) and energy consumption (b) of various vacuum levels in 10 bar VPSA processes.

- Both purities and recoveries of products benefit from the deeper vacuum, but more energy is required.
- There is a tradeoff between separation performance and energy consumption.

Separation performance_30 bar PSA

- Step configuration: 5-bed PSA process, 10 steps each cycle

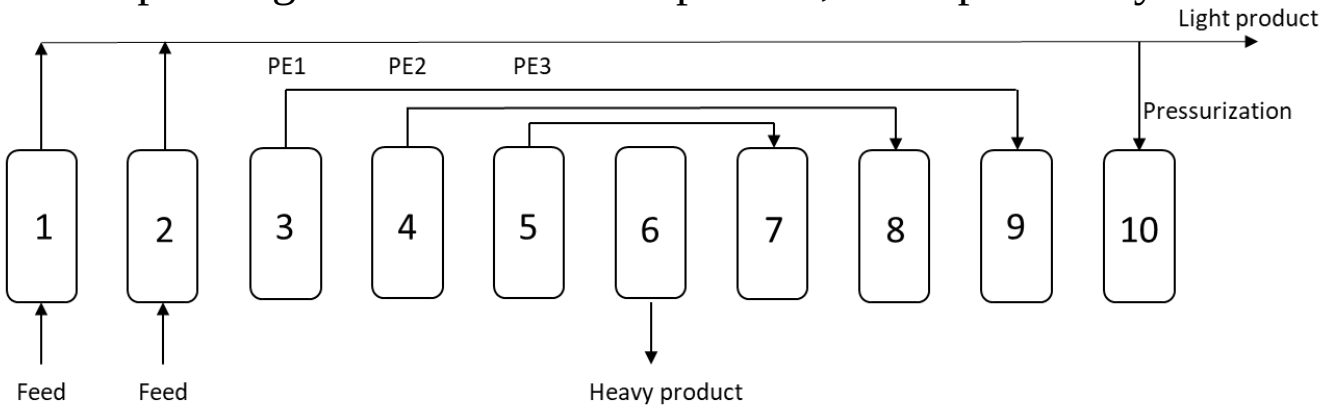

- Inlet pressure = 30 bar, desorption pressure = 1 bar – No energy required for vacuum

Physical size (m)	Feed H_2 concentration (%)	H_2 downstream concentration (%)	CH_4 topstream concentration (%)	H_2 recovery rate (%)	CH_4 recovery rate (%)	Energy consumption (kJ/kg CH_4)
	3	6.59	99.01	78.90	65.44	0
	4	7.96	99.05	86.52	58.33	0
0.3 x 1.8	5	9.17	98.98	89.61	53.27	0
	10	15.27	98.95	96.13	40.74	0
	15	19.79	99.08	73.85	31.43	0

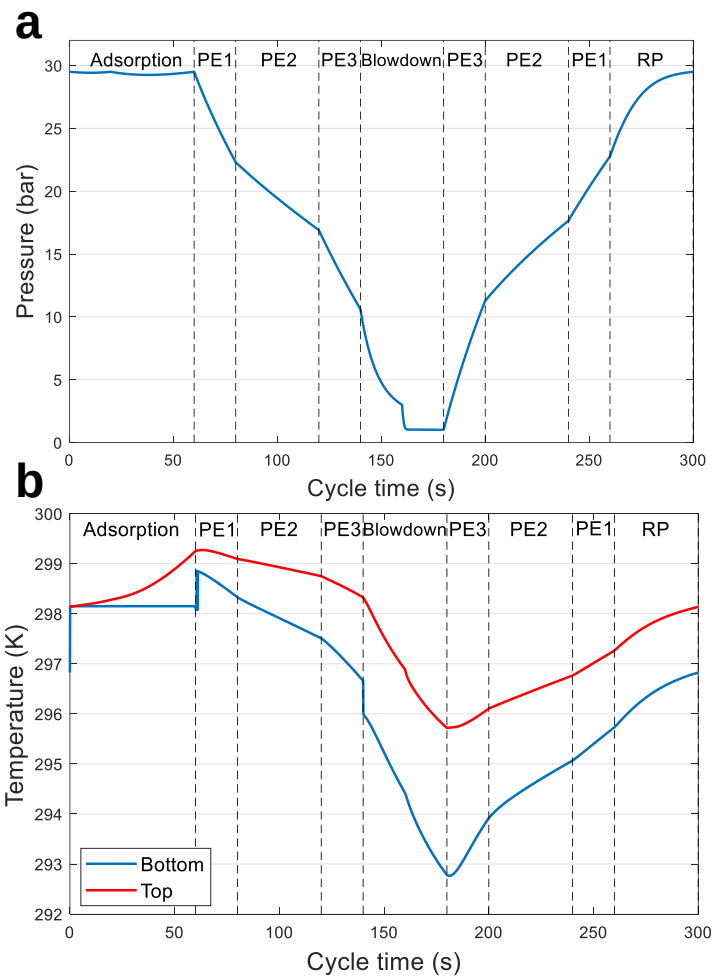

Example pressure profile (a) and temperature profile (b) of 30 bar PSA process over one cycle at cyclic steady state condition (Feed H_2 concentration = 5%).

Separation performance_50 bar PSA

- Step configuration: 6-bed PSA process, 12 steps each cycle

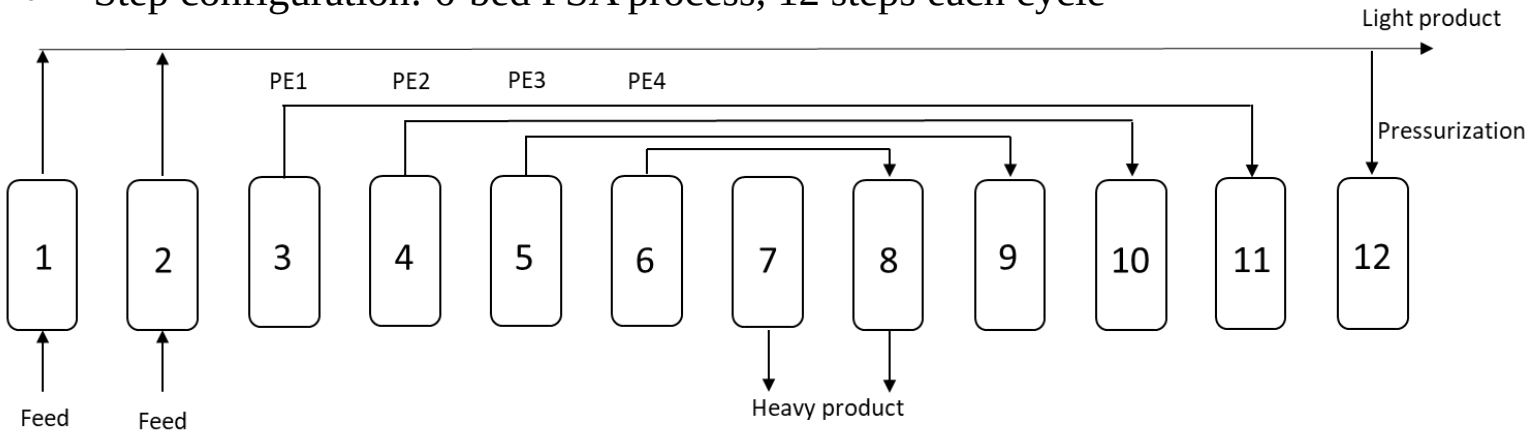

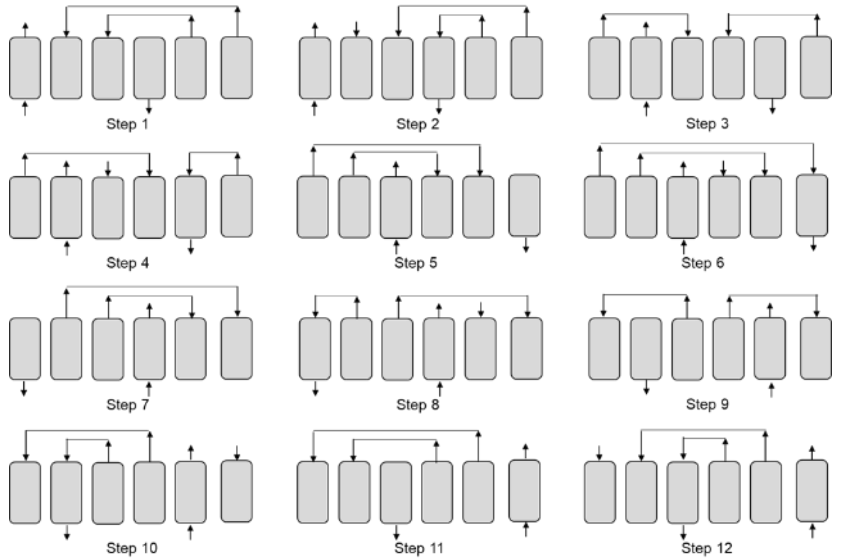

- Inlet pressure = 50 bar, desorption pressure = 1 bar – No energy required for vacuum

Physical size (m)	Feed H_2 concentration (%)	H_2 downstream concentration (%)	CH_4 topstream concentration (%)	H_2 recovery rate (%)	CH_4 recovery rate (%)	Energy consumption (kJ/kg CH_4)
0.3 x 1.8	3	6.36	98.95	77.97	64.54	0
	4	7.82	98.92	84.80	58.37	0
	5	8.98	99.00	90.11	51.91	0
	10	13.80	99.01	97.12	32.56	0
	15	17.54	98.99	99.03	17.84	0

Zeolite 3A vs activated carbon

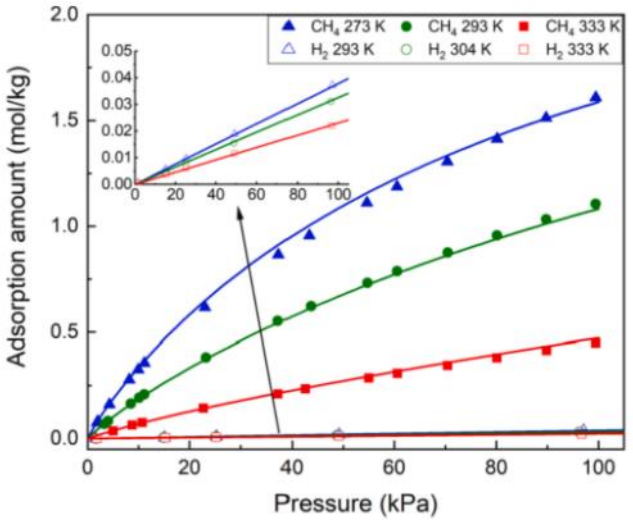

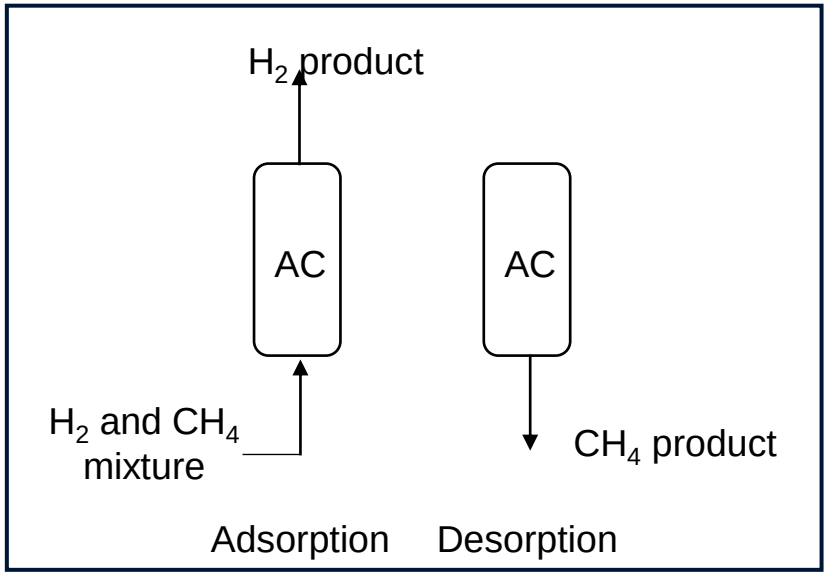

Parameters in the Langmuir model for H_2 and CH_4 adsorption on activated carbon

Component	m_i (mol/kg)	n_i (mol/kg)	b_0 (1/kPa)	d_0 (1/kPa)	Q_{1i} (J/mol)	Q_{2i} (J/mol)
CH_4	8.49E-02	2.97	7.26E-05	2.64E-07	17.66	24.01
H_2	4.90	-	1.24E-06	-	10.10	-

Dehdari, L., et al., *Separation of hydrogen from methane by vacuum swing adsorption.* Chemical Engineering Journal, 2022. **450**: p. 137911.

Activated carbon PSA

- Feed hydrogen concentration = 5%: 5-bed H_2 PSA cycle with 4 pressure equalizations (PEs) steps

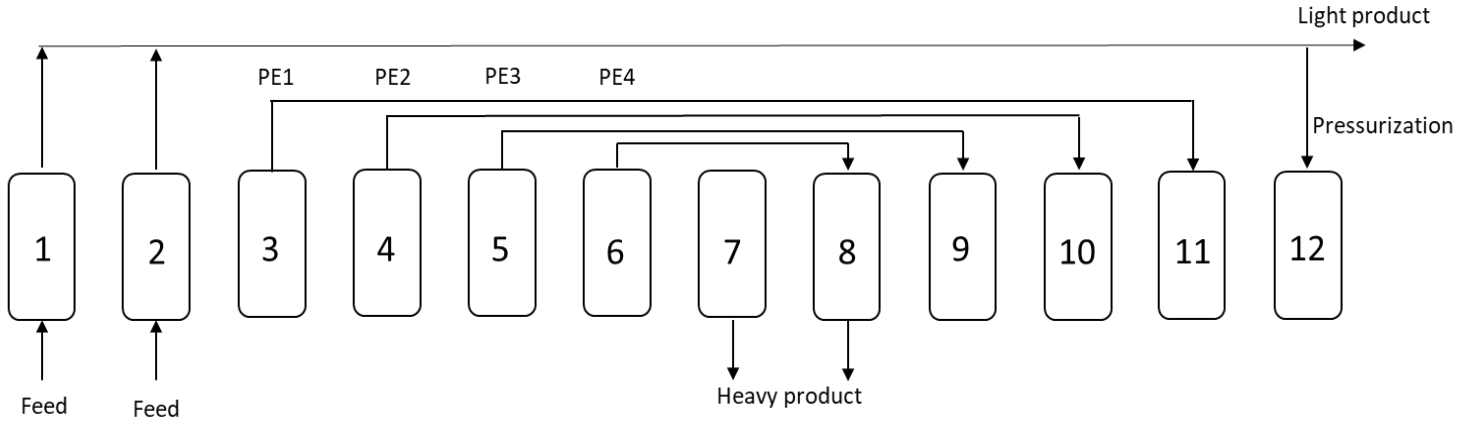

- Feed hydrogen concentration = 10 & 15%: 5-bed H_2 PSA cycle with CH_4 product purge step

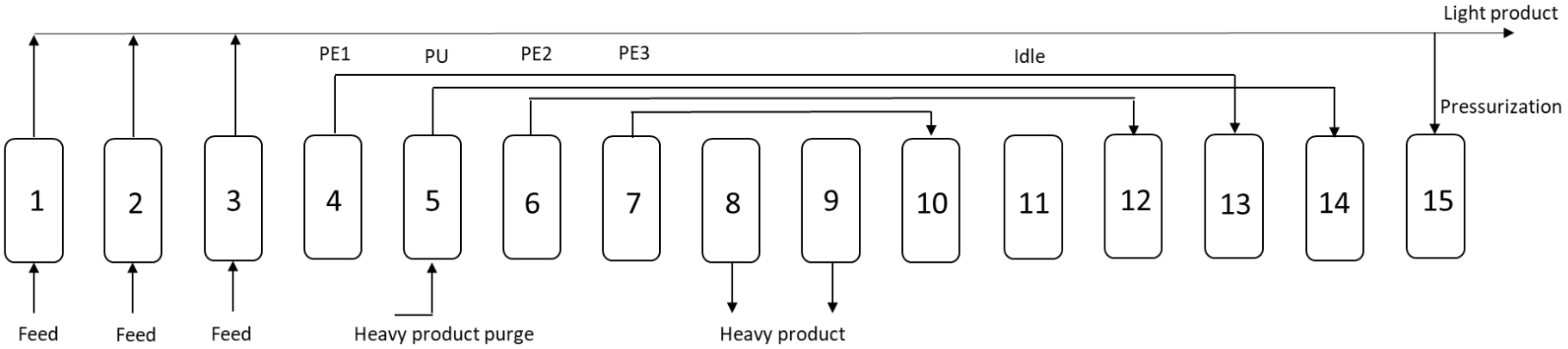

Zeolite 3A vs activated carbon

- Feed gas: 100 m^3/h = 1.24 mol/s
- Feed gas pressure: 30 bar
- Design: 5 bed PSA
- Physical size: 0.3 x 1.8 m

Adsorbent	Feed H_2 concentration (%)	CH_4 topstream concentration (%)
Zeolite 3A	5	98.98
	10	98.95
	15	99.08

Adsorbent	Feed H_2 concentration (%)	CH_4 downstream concentration (%)
Activated carbon	5	99.14
	10	98.98
	15	98.94

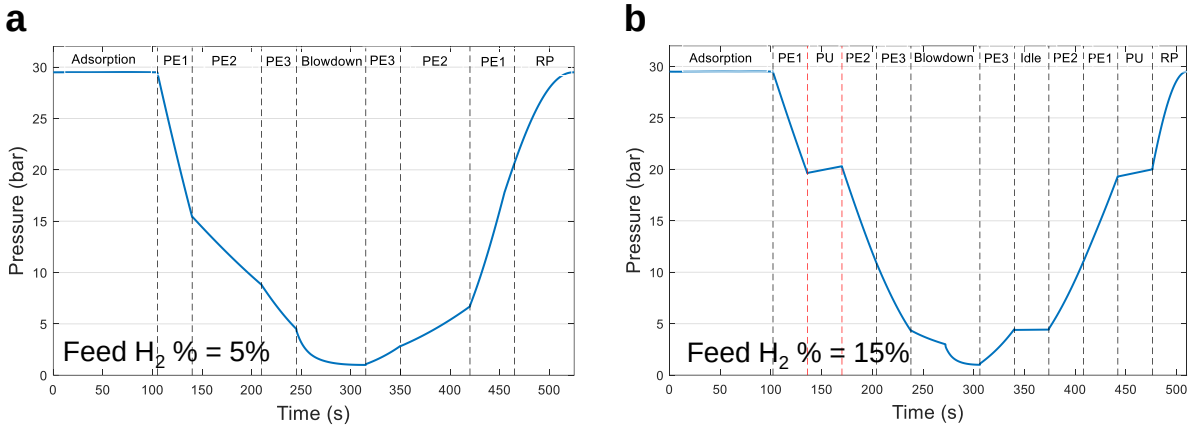

Pressure profiles of 5% (a) and 15`% (b) feed hydrogen concentration activated carbon PSA systems as a function of cycle time. (Adsorption pressure = 30 bar.)

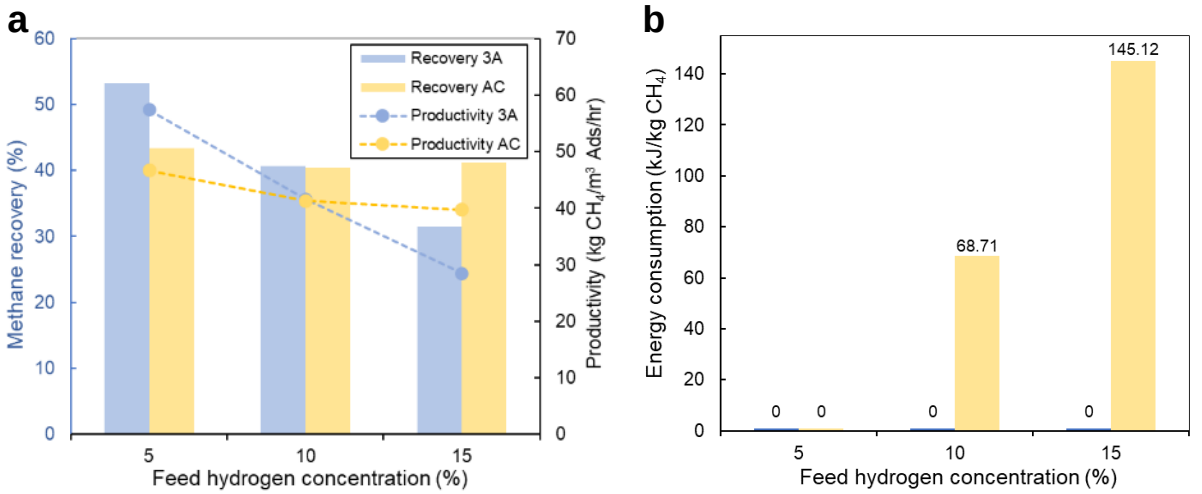

Comparison between activated carbon and zeolite 3A in terms of recovery, productivity (a) and power consumption (b). (Adsorption pressure = 30 bar.)

Tech 1 summary

- Zeolite 3A is one of only a few adsorbents that can selectively adsorb H_2 and can be used for H_2 capture from blended pipeline gas using PSA processes at room temperature.

- The designed PSA system shows promising technical feasibility to produce a high purity CH_4 product (>99%) using zeolite 3A adsorbent.

- Zeolite 3A has advantages over activated carbon for the same separation configuration in terms of recovery, productivity and energy consumption especially when the feed H_2 concentration is low (≤10%).

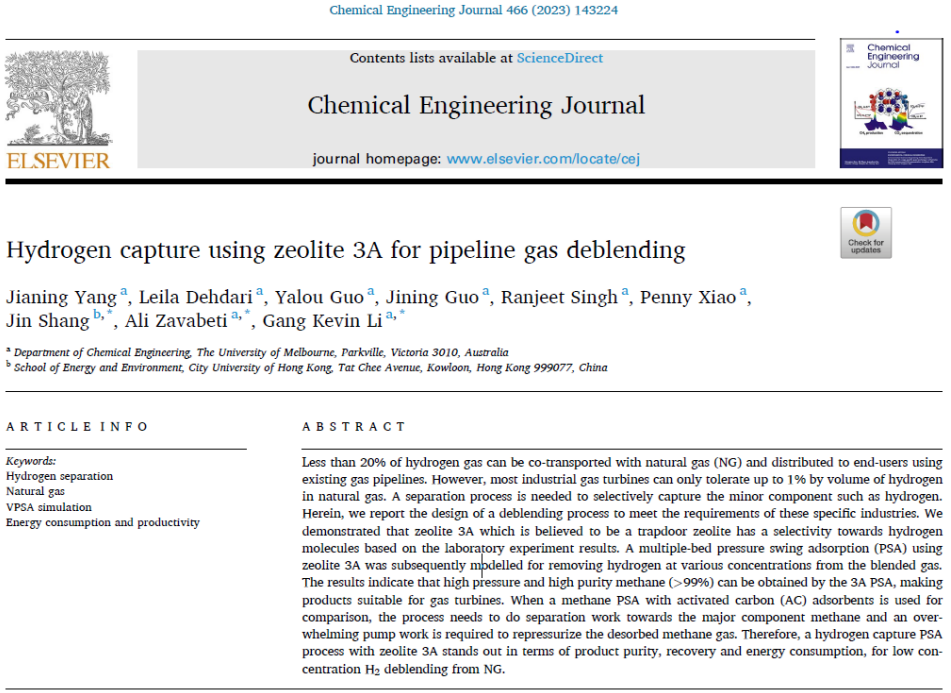

Chemical Engineering Journal 466 (2023) 143224

Contents lists available at ScienceDirect

Chemical Engineering Journal

journal homepage: www.elsevier.com/locate/cej

Hydrogen capture using zeolite 3A for pipeline gas deblending

Jianing Yang [a], Leila Dehdari [a], Yalou Guo [a], Jining Guo [a], Ranjeet Singh [a], Penny Xiao [a], Jin Shang [b,*], Ali Zavabeti [a,*], Gang Kevin Li [a,*]

[a] Department of Chemical Engineering, The University of Melbourne, Parkville, Victoria 3010, Australia
[b] School of Energy and Environment, City University of Hong Kong, Tat Chee Avenue, Kowloon, Hong Kong 999077, China

ARTICLE INFO

Keywords:
Hydrogen separation
Natural gas
VPSA simulation
Energy consumption and productivity

ABSTRACT

Less than 20% of hydrogen gas can be co-transported with natural gas (NG) and distributed to end-users using existing gas pipelines. However, most industrial gas turbines can only tolerate up to 1% by volume of hydrogen in natural gas. A separation process is needed to selectively capture the minor component such as hydrogen. Herein, we report the design of a deblending process to meet the requirements of these specific industries. We demonstrated that zeolite 3A which is believed to be a trapdoor zeolite has a selectivity towards hydrogen molecules based on the laboratory experiment results. A multiple-bed pressure swing adsorption (PSA) using zeolite 3A was subsequently modelled for removing hydrogen at various concentrations from the blended gas. The results indicate that high pressure and high purity methane (>99%) can be obtained by the 3A PSA, making products suitable for gas turbines. When a methane PSA with activated carbon (AC) adsorbents is used for comparison, the process needs to do separation work towards the major component methane and an overwhelming pump work is required to repressurize the desorbed methane gas. Therefore, a hydrogen capture PSA process with zeolite 3A stands out in terms of product purity, recovery and energy consumption, for low concentration H_2 deblending from NG.

Yang, J., Dehdari, L., Guo, Y., Guo, J., Singh, R., Xiao, P., ... & Li, G. K. (2023). Hydrogen capture using zeolite 3A for pipeline gas deblending. *Chemical Engineering Journal*, *466*, 143224.

2 - Recovery of low-concentration hydrogen using alloy $LaNi_5$ based pressure swing adsorption

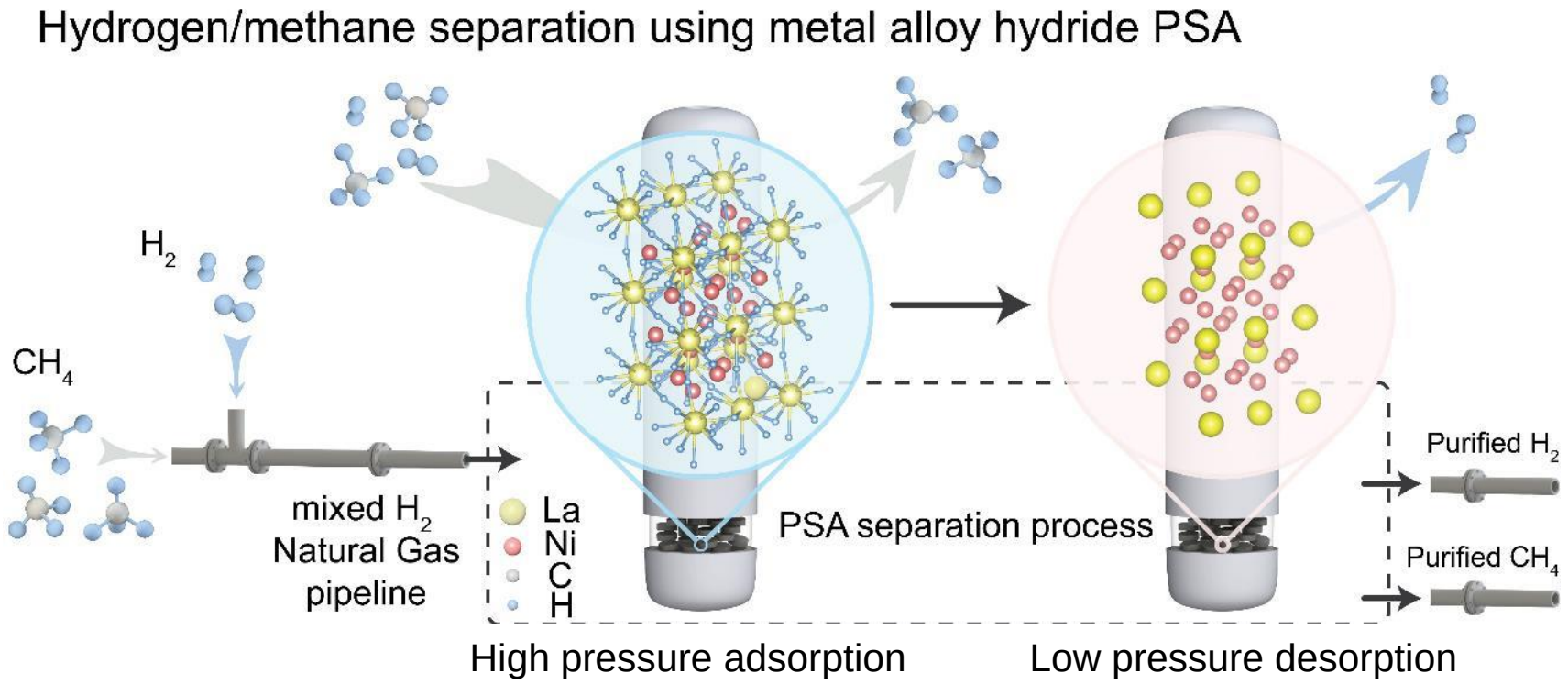

Mechanism of hydrogen adsorption on $LaNi_5$

- Metal alloys are candidate materials for hydrogen storage. Hydrogen adsorption/desorption reactions can be written according to following equation, including the heat of reaction:

$$M + (x/2)H_2 \leftrightarrow MH_x + \Delta H_{adsorption}$$

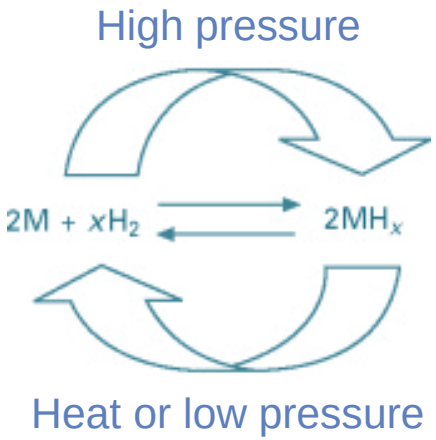

Mechanism of hydrogen adsorption on $LaNi_5$

1) External diffusion and physisorption - H_2 from surrounding diffuses to the external surface of MHy (β phase);
2) Dissociative chemisorption - H_2 dissociate and chemisorb on the surface of MH;
3) Internal diffusion - H atoms penetrate the ash layer and reached the external surface of MHx (α phase);
4) Chemical reaction - H atoms react on the surface MHx (α phase) and generate a new ash layer MHy (β phase).

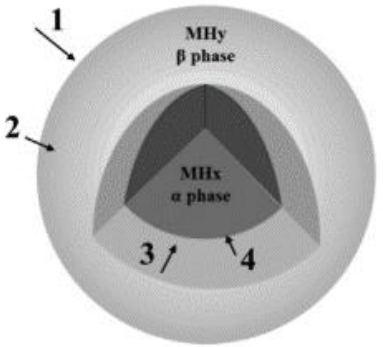

Li, D., Wang, Y., Wu, L., Yang, F., Wu, Z., Zheng, L., ... & Zhang, Z. (2020). Kinetics study on the nonlinear modified varying-size model of LaNi5 during hydrogenation/dehydrogenation. *Chemical Engineering Science*, *214*, 115439.

Adsorption isotherms

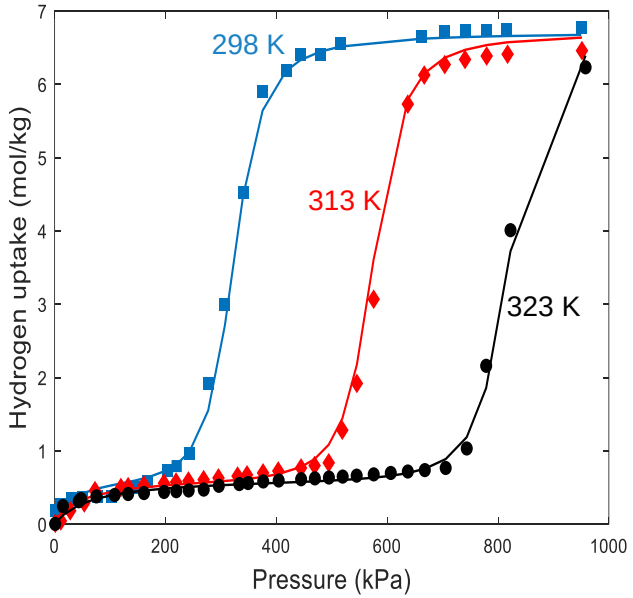

Adsorption isotherms of H_2 on $LaNi_5$ at different temperatures. Lines – Rutherford Extended CMMS model and symbols – experimental data

- $LaNi_5$ can work at moderate temperatures and pressures.
- The capacity of $LaNi_5$ alloy is high (up to 6.8 mol/kg).
- As the temperature increases, the plateau pressure also increases because an increase in temperature favors the endothermic desorption of hydrogen.

- Rutherford Extended CMMS model

$$q^*_{H_2} = \frac{C_{sat} k_{0T} \exp(\frac{q_0}{RT}) P}{k_{0T} \exp\left(\frac{q_0}{RT}\right) P + w^2} + \frac{C_{satL} b_{LT} \exp(\frac{q_L}{RT}) P}{1 + b_{LT} \exp(\frac{q_L}{RT}) P}$$

$$w = \frac{1}{2}(1 - k_{1T} \exp(\frac{q_1}{RT}) P + \sqrt{(1 - k_{1T} \exp(\frac{q_1}{RT}) P)^2 + 4 k_{0T} \exp(\frac{q_0}{RT}) P})$$

- Parameters in the CMMS equation

Parameters	Value	Unit
C_{sat}	6.09	mol/kg
K_{0t}	6.60E-20	1/kPa
Q_0	82884	J/mol
C_{satL}	0.63	mol/kg
B_{Lt}	7.87E-07	1/kPa
Q_L	26654	J/mol
K_{1t}	1.86E-08	kPa
Q_1	29791	J/mol

Reaction kinetics

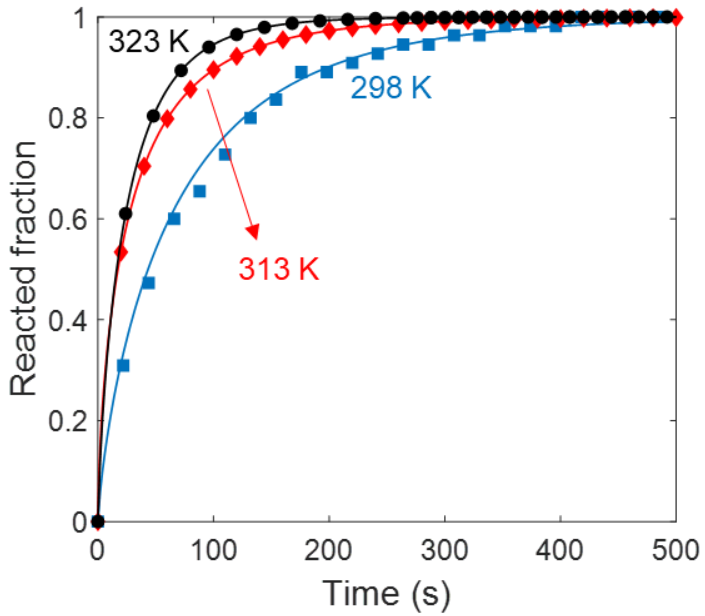

Experimental data (symbols) and JMA model simulation curves (lines) at 30 bar and three different temperatures.

- Reaction kinetics were measured at different temperatures at 30 bar.
- The hydriding reaction rates increase with operating temperatures.

- The hydriding kinetics are analyzed using the JMA model.

$$f(t) = \frac{q_{H_2}}{q^*_{H_2}} = 1 - \exp(-kt^n)$$

$$k = A \times \exp\left(-\frac{E_a}{RT}\right)$$

- Parameters in the JMA model for H_2 adsorption on $LaNi_5$

Parameters	Value	Unit
Activation energy (Ea)	24.803	kJ/mol H_2
Preexponential factor (A)	785.38	s^{-1}
Order of reaction (n)	1	/

$LaNi_5$ material characterizations

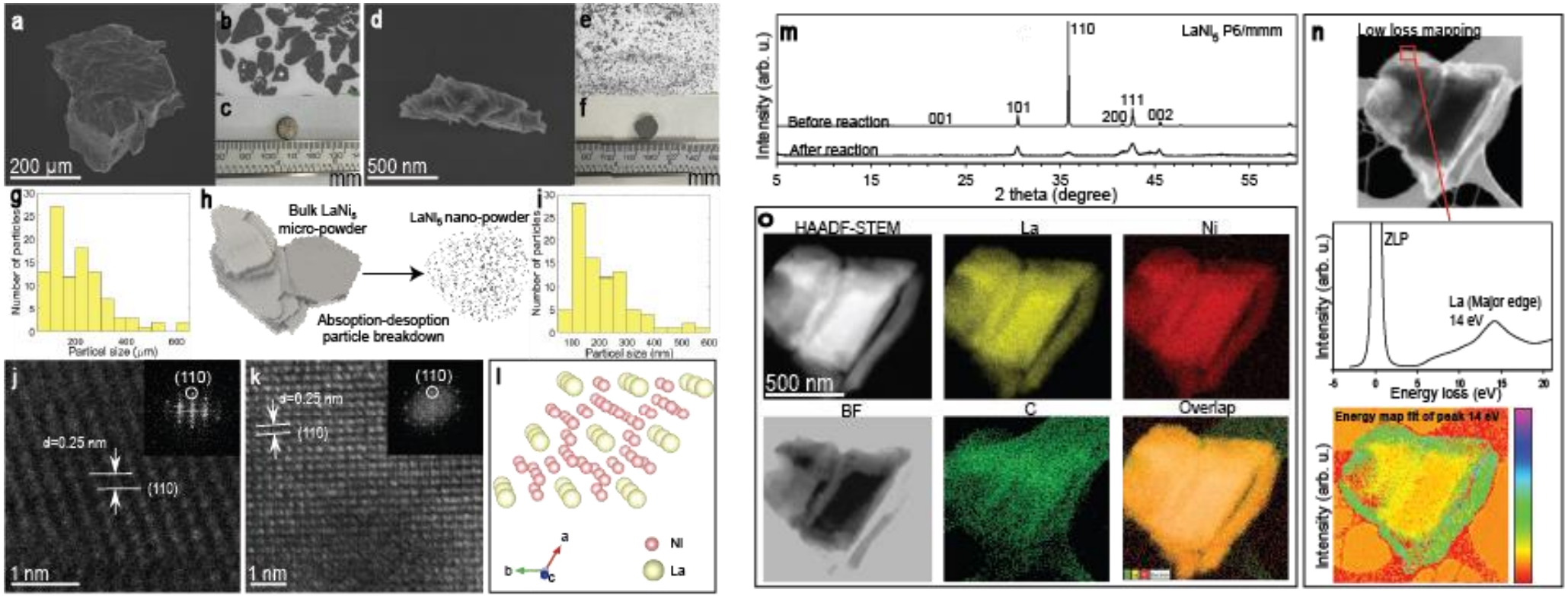

$LaNi_5$ alloy characterization. Pre-adsorption micro-powder precursor, a) SEM micrograph, b) optical image, and c) created packing and post-adsorption naturally formed nano-powder, d) SEM and e) optical microscopy images, and f) corresponding formed pellet, g, h) revealing the size distribution and schematic representation of the initial powder precursor and h, i) elucidating size-morphology transition to nano-sized powder. j) and k) HRTEM images of precursor and post-adsorption powder. l) schematic presentation of $LaNi_5$ the crystal structure with projection of. m) Powder XRD pattern of samples before adsorption and after desorption, n) TEM-based Electron energy loss micrograph of a sample after desorption is generated from the low-loss region. Below is the low-loss energy region spectrum, integrated over the shown area of the micrograph with negligible distinction from the sample before adsorption. o) elucidates the sample's corresponding TEM-EDX mapping with colour maps of La and Ni elemental distribution.

Experiment validation

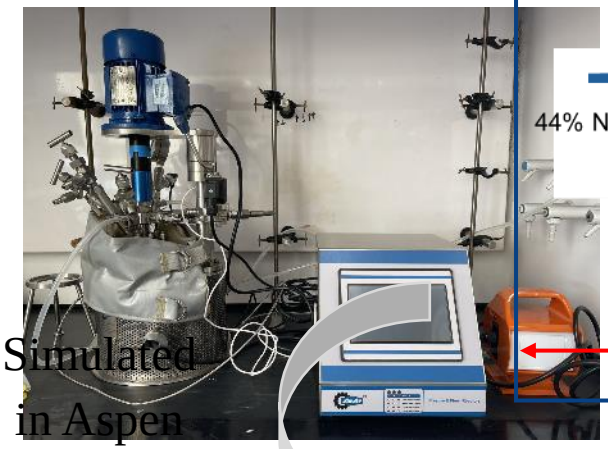

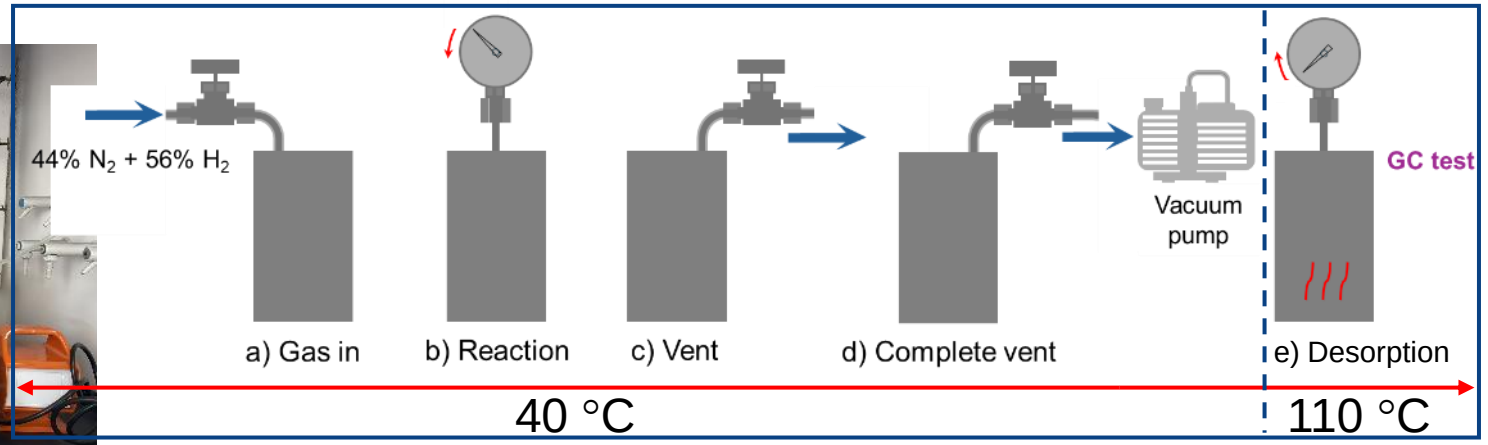

Simulated in Aspen Adsorption software

- Step a): Gas in (N_2+H_2)
- Step b): Reaction
- Step c): Vent (1 bar)
- Step d): Complete vent
- Step e): Desorption

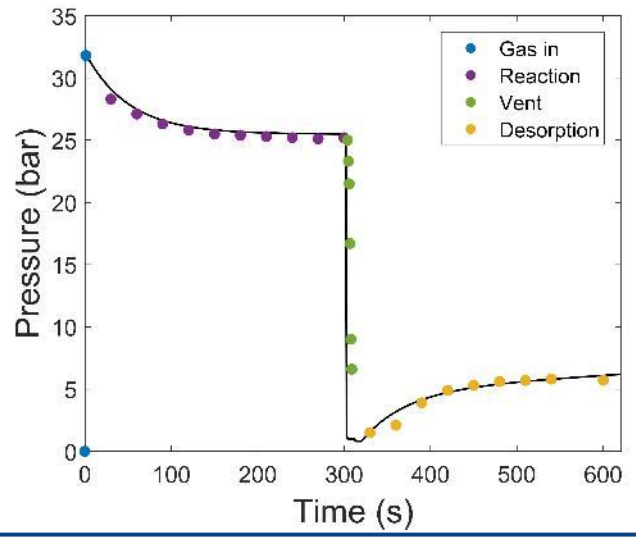

Experiment results vs simulation results

Gas sample	Desorption gas
H_2% from GC test	96.57
H_2% from simulation	98.41

- Both N_2 and CH_4 are not adsorbed by $LaNi_5$, so for safety reasons, N_2 was used instead of CH_4 in the experiment.

VPSA design

VPSA column and $LaNi_5$ characteristics used in the simulation

Parameter	Value	Unit
Inlet pressure	30	bar
Vacuum pressure	0.35	bar
Column height	1	m
Column diameter	0.02	m
Inter-particle voidage	0.33	m^3 void/m^3 bed
Intra-particle voidage	0.248	m^3 void/m^3 bead
Particle radius	2	mm
Bulk solid density of adsorbent	3354.9	kg/m^3
Temperature	313	K
Flowrate	6, 8, 10, 12	st.L/min

Separation step configuration

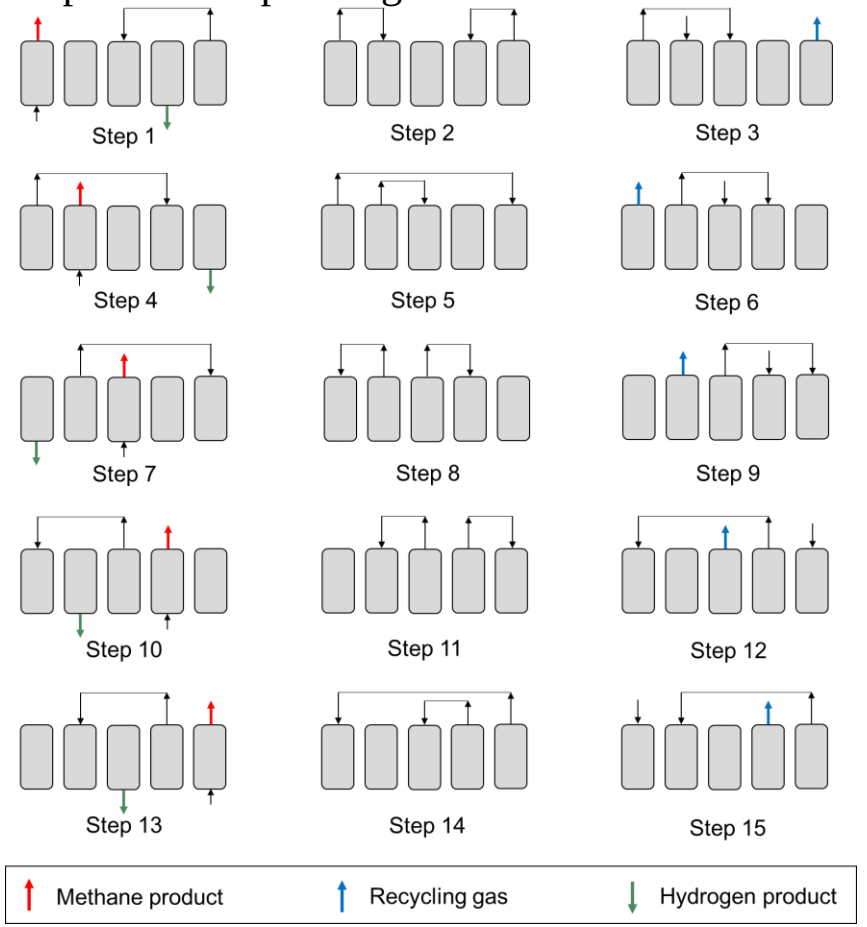

Column \ Step	1	2	3	4	5	6	7	8	9	10	11	12	13	14	15
1	AD	PE1	PE2	PE3	PE4	Vent	VAC	RPE4	Idle	RPE3	Idle	RPE2	IDLE	RPE1	RP
2	Idle	RPE1	RP	AD	PE1	PE2	PE3	PE4	Vent	VAC	RPE4	Idle	RPE3	Idle	RPE2
3	RPE3	Idle	RPE2	Idle	RPE1	RP	AD	PE1	PE2	PE3	PE4	Vent	VAC	RPE4	Idle
4	VAC	RPE4	Idle	RPE3	Idle	RPE2	Idle	RPE1	RP	AD	PE1	PE2	PE3	PE4	Vent
5	PE3	PE4	Vent	VAC	RPE4	Idle	RPE3	Idle	RPE2	Idle	RPE1	RP	AD	PE1	PE2

Flowrate determination (feed hydrogen concentration = 10%)

Outlet gas	Concentration (%)	Recovery (%)	Adsorption time /cycle time (s)	Flowrate (st.L/min)	Energy consumption (kJ/kmol CH_4)
Topstream CH_4	99.08	96.49	460+15+15	4	124.56
Downstream H_2	98.27	88.76	2450		
Recycling gas (H_2)*	11.20	3.16			
Topstream CH_4	99.07	96.69	340+15+15	6	123.39
Downstream H_2	98.70	88.46	1850		
Recycling gas (H_2)*	12.72	3.30			
Topstream CH_4	99.10	95.78	240+15+15	8	125.19
Downstream H_2	98.35	88.38	1350		
Recycling gas (H_2)*	10.30	3.69			
Topstream CH_4	99.04	95.95	170+15+15	10	123.32
Downstream H_2	98.23	87.37	1000		
Recycling gas (H_2)*	12.43	4.19			
Topstream CH_4	99.04	93.09	100+15+15	12	126.15
Downstream H_2	96.91	85.50	650		
Recycling gas (H_2)*	10.71	6.32			

*Recycling gas contains mixed gases, and in the table, the purity and recovery are recorded for H_2 content within the stream

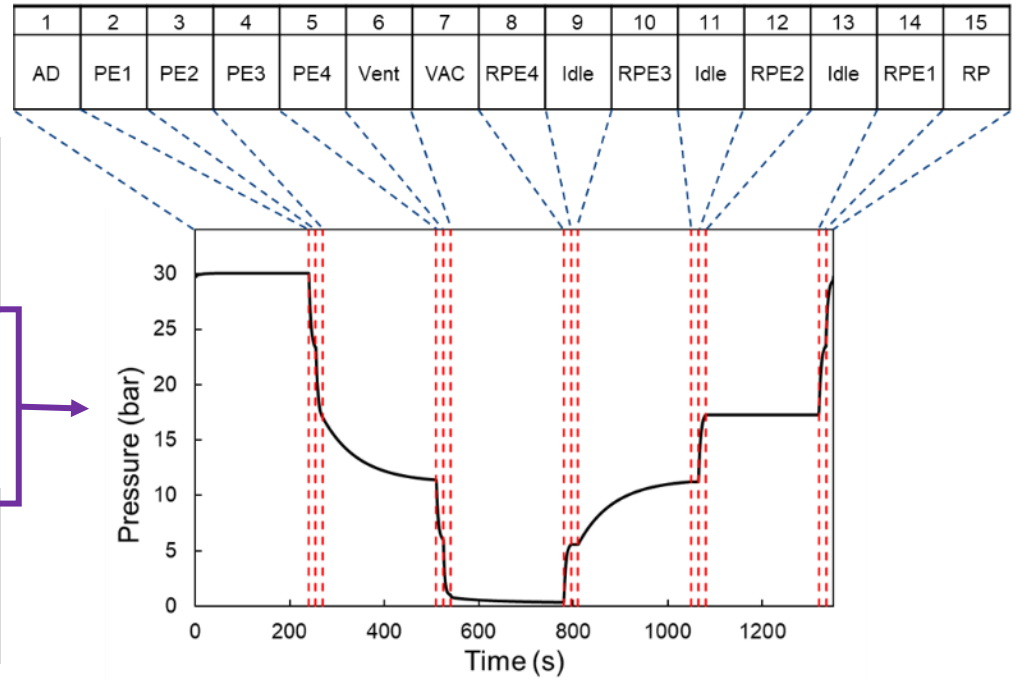

Pressure profile of VPSA process in one cycle for feed hydrogen concentration of 10 % and flow rate of 8 st.L/min.

Separation performance (flowrate = 8 st.L/min)

Inlet gas		Outlet gas	Purity (%)	Recovery (%)	Cycle time (s)	Energy consumption (kJ/kmol CH_4)
CH_4	95%	Topstream CH_4	99.02	97.88		
H_2	5%	Downstream H_2	96.94	77.06	2125	51.20
		Recycling gas (H_2)*	10.90	4.44		
CH_4	90%	Topstream CH_4	99.10	95.78		
H_2	10%	Downstream H_2	98.35	88.38	1350	125.19
		Recycling gas (H_2)*	10.30	3.69		
CH_4	85%	Topstream CH_4	98.98	94.63		
H_2	15%	Downstream H_2	99.43	88.98	1150	199.78
		Recycling gas (H_2)*	15.44	5.56		
CH_4	80%	Topstream CH_4	99.07	90.91		
H_2	20%	Downstream H_2	99.35	91.22	750	302.94
		Recycling gas (H_2)*	13.43	5.45		

*Recycling gas contains mixed gases, and in the table, the purity and recovery are recorded for H_2 content within the stream

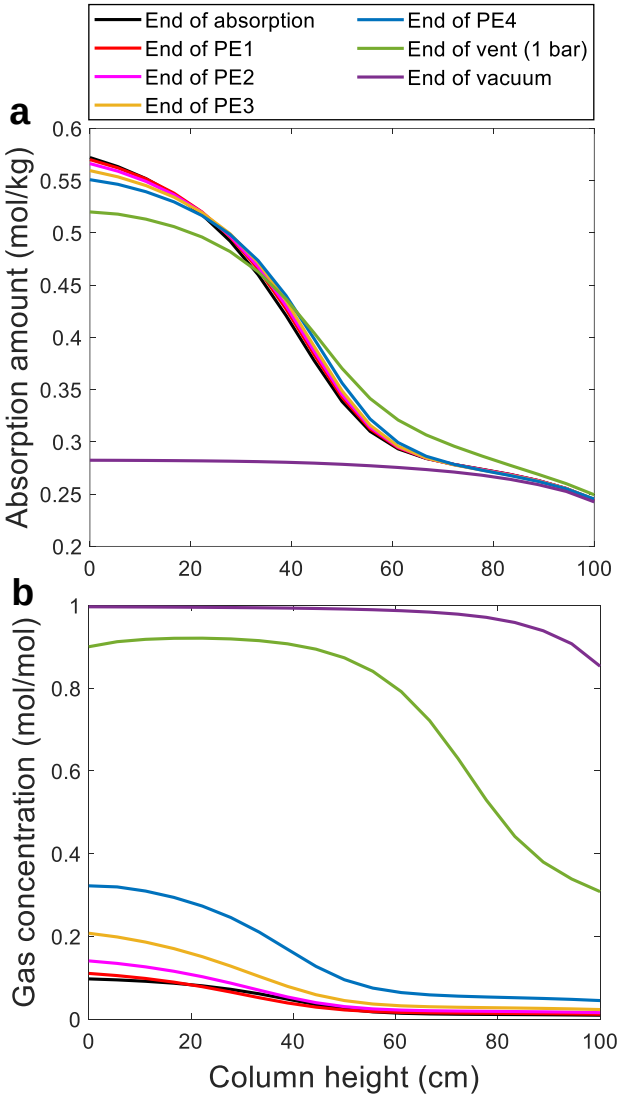

Hydrogen concentration profile in solid phase (a) and gas phase (b) against location in column.

Tech 2 summary

- $LaNi_5$ exhibits fast reaction kinetics and high hydrogen adsorption capacity at moderate temperatures and pressures.
- The experiment results demonstrate that hydrogen can be successfully captured and separated by $LaNi_5$ using an autoclave pressure vessel.
- The designed multiple bed vacuum pressure swing adsorption (VPSA) process has been modeled with the validated Aspen Adsorption simulation tool.
- High purity hydrogen products and methane products (both >99%) can be obtained from the designed VPSA process with high recovery exceeding 90% when the feed hydrogen concentration is 20%.

Contents lists available at ScienceDirect

Chemical Engineering Journal

journal homepage: www.elsevier.com/locate/cej

Recovery of low-concentration hydrogen using alloy $LaNi_5$ based pressure swing adsorption

Jianing Yang [a], Ali Zavabeti [a,b], Yalou Guo [a,c], Zhi Yu [a], Leila Dehdari [a], Jining Guo [a], Chao Wu [a], Dingqi Wang [a], Jia Ming Goh [a], Penny Xiao [a], Gang Kevin Li [a,*]

[a] Department of Chemical Engineering, The University of Melbourne, Parkville, Victoria 3010, Australia
[b] Department of Chemical Engineering, RMIT University, Melbourne, Victoria 3001, Australia
[c] Department of Chemical Engineering, Monash University, Clayton, Victoria 3800, Australia

ARTICLE INFO

Keywords:
Hydrogen separation
Natural gas
VPSA simulation
Metal hydride

ABSTRACT

A cost-effective strategy for long distance hydrogen transportation entails its integration into existing natural gas pipelines. The demand for efficient separation of the minor component hydrogen poses a challenge for post co-transportation gas treatment to meet the specifications of various industrial applications. While porous materials for selective H_2 adsorption are extremely rare, certain metal alloys known for their hydrogen storage property via reversible hydriding/dehydriding reaction show great promise for selective H_2 separation. Despite the unfavorable and harsh reaction conditions of most metal hydrides, $LaNi_5$ displays unique H_2 adsorption properties at moderate temperatures and pressures, rendering it a promising material for hydrogen separation. Our experimental measurements reveal that $LaNi_5$ exhibits rapid H_2 update kinetics and a high adsorption capacity of 6.8 mol/kg at 25 °C and 600 kPa. Preliminary experiments based on a single pressure vessel were conducted to demonstrate that hydrogen gas can be successfully enriched from 56 % to 96.57 % via a roundtrip (adsorption and desorption) process. To explore the full potential of this process, a pressure swing hydride process akin to classical vacuum pressure swing adsorption (VPSA) was designed to recover the minor component H_2 from the mixture, achieving high-purity CH_4 and H_2 (both >99 %) products at the same time with recoveries exceeding 90 %. The findings of this study underscore the feasibility and efficacy of metal hydride pressure swing adsorption to generate high-purity hydrogen and methane gases for the energy industry.

Yang, J., Zavabeti, A., Guo, Y., Yu, Z., Dehdari, L., Guo, J., ... & Li, G. K. (2024). Recovery of low-concentration hydrogen using alloy $LaNi_5$ based pressure swing adsorption. *Chemical Engineering Journal*, *493*, 152395.

3 – High purity helium and hydrogen production from natural hydrogen mines

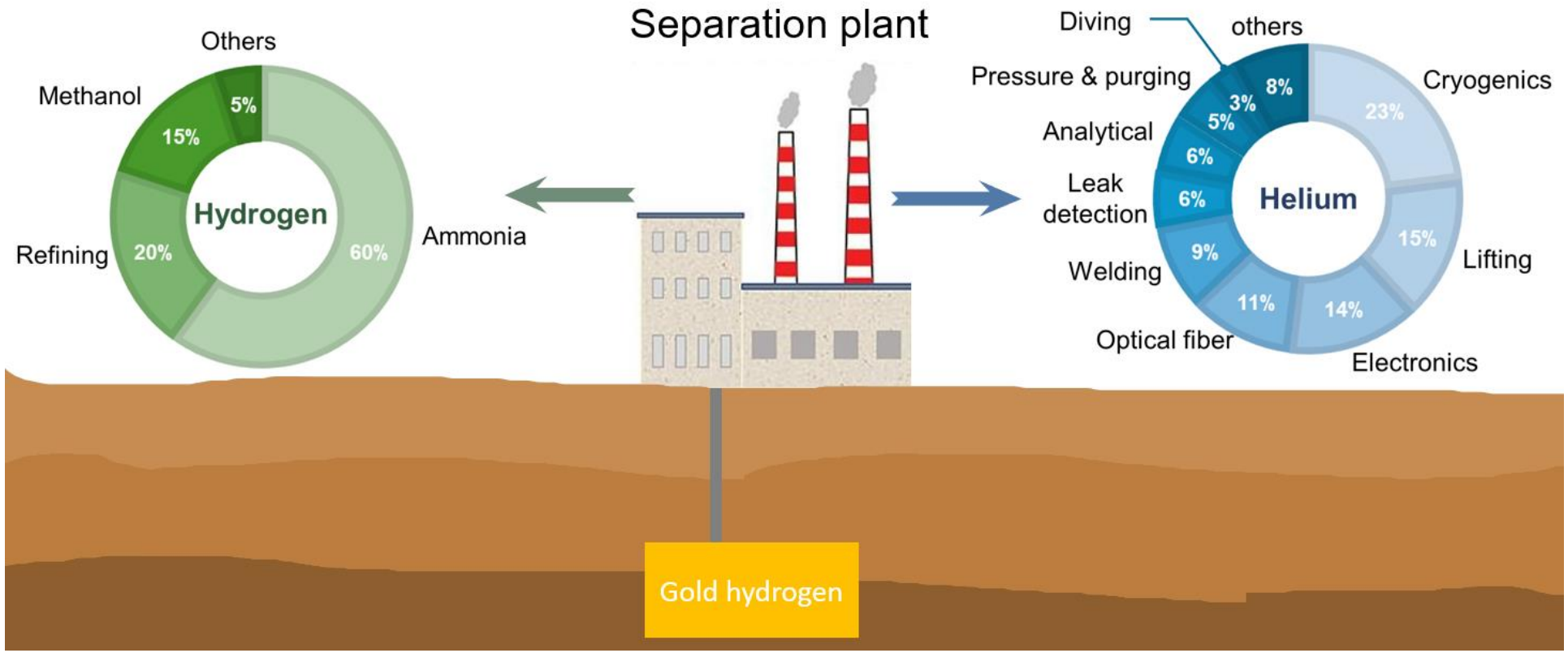

Background-Helium Production

- The helium separation and purification is commonly done via cryogenic distillation, which is cost and energy intensive technology.
- For a higher energy efficiency the potential of several emerging technologies based on adsorption and/or membrane separation have been investigated.

Currently, cryogenic separation is the only method used for large-scale helium recovery.

Followed by pressure swing adsorption (PSA) for further upgrading (purity higher than 90%).

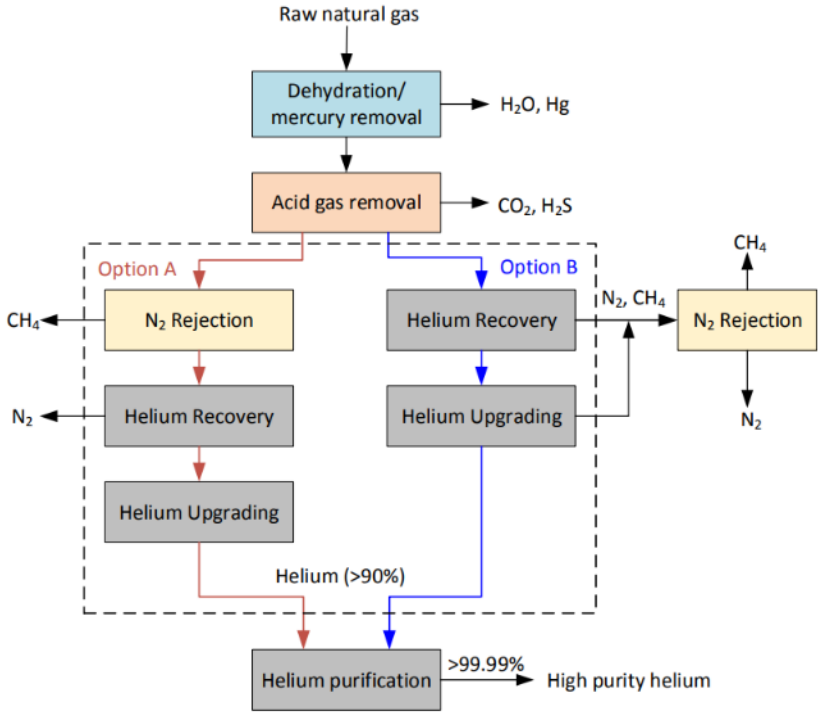

Process illustration of helium production from natural gas

Helium Cryogenic Gas Purification Systems from Ability Engineering

Rufford, T. E., Chan, K. I., Huang, S. H., May, E. F., 2014, A Review of Conventional and Emerging Process Technologies for the Recovery of Helium from Natural Gas, Adsorption Science & Technology 32 (1), 49– 72. DOI: 10.1260/0263-6174.32.1.49
Liemberger, W., Miltner, M., & Harasek, M. (2018). Efficient extraction of helium from natural gas by using hydrogen extraction technology. *Chemical Engineering Transactions*, *70*, 865-870..

Hydrogen resources

Colors to distinguish between different kinds of hydrogen:

- **Gray hydrogen** Made from fossil fuels, which release carbon dioxide and add to global warming.
- **Blue hydrogen** Same as gray hydrogen, but the carbon is captured and sequestered.
- **Green hydrogen** Made without carbon emissions by using renewable electricity to split water.
- **Orange hydrogen** Stimulated by pumping water into deep source rocks.
- **Gold hydrogen** Tapped from natural subsurface accumulations.

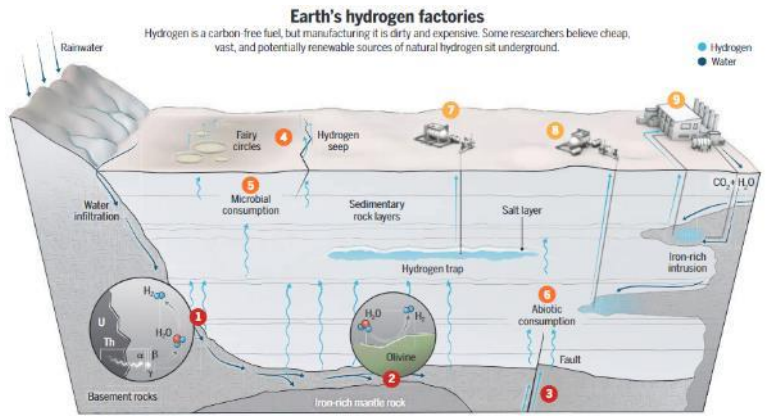

Hand, E. (2023). Hidden hydrogen. *Science (New York, NY)*, *379*(6633), 630-636.

$LaNi_5$ with high H_2 adsorption capacity can be used to separate H_2/He mixtures to obtain high purity H_2 and He products.

Gold Hydrogen

19 December 2023
ASX Announcement

Ramsay 2 Update

Very High Hydrogen Concentrations up to 86% Purity Found Along with the Very High Helium Concentrations

Key Highlights:

1. **Completion of Ramsay 2 Well:**
   - On 1 December, 2023, Ramsay 2 achieved its final Total Depth (TD) of 1068mMD. Logging operations have been successfully completed, and casing has been securely cemented in place.
2. **Very High Hydrogen Concentrations up to 86%**
   - Post drill analysis of the mudgas samples and the calibrated real time mudgas log data reveal very high air-corrected hydrogen concentrations, reaching up to 86% at shallow levels from 194m through to 536m in the Parara and Kulpara formations.
   - These measurements validate the historic results from Ramsay Oil Bore 1 (1931) and confirm the presence of a hydrogen play at shallow depths in the Ramsay Project Area which aligns very closely with the results of Ramsay 1 (October 2023).
   - Mud gas data, calibrated with isotube analysis, shows the fractured granitic basement contains significant levels of hydrogen within the open fractures, in line with pre-drill model underpinning the prospective resource assessment.
   - Flow testing of completed wells will ultimately confirm hydrogen concentrations, flow rates, and hence the commerciality of the hydrogen play.

Drilling at Ramsay 2 commenced on 17 November 2023, and was completed at a total depth of 1068m with all well activities finalized on 1 December 2023.

- Very High Hydrogen Concentrations up to **86%.**
- World-Class Helium Concentrations of **6.8%** raw gas.[35]

Proof of concept – selectivity to hydrogen

- 10 bar helium gas was initially introduced into the pressure vessel and the pressure within the vessel remained unchanged.
- 30 bar hydrogen gas was injected, resulting in a significant pressure drop. This experiment demonstrates that the material $LaNi_5$ exhibits strong selectivity towards hydrogen, making it suitable for hydrogen capture and separation.

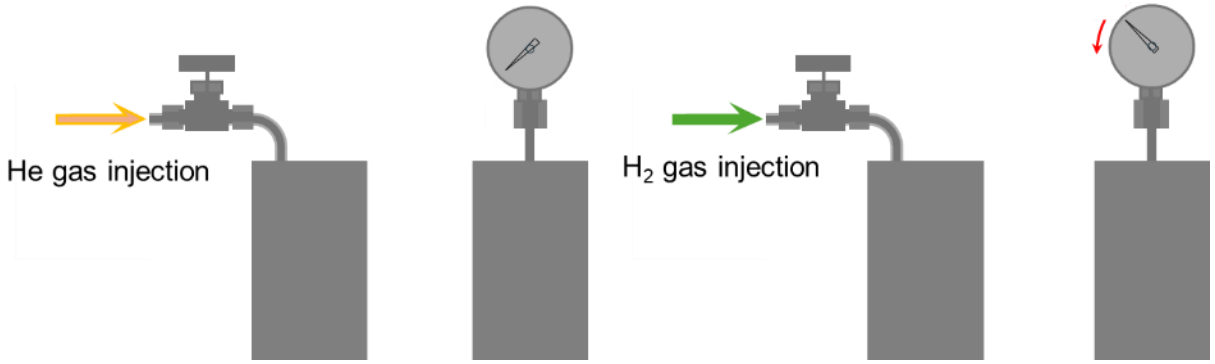

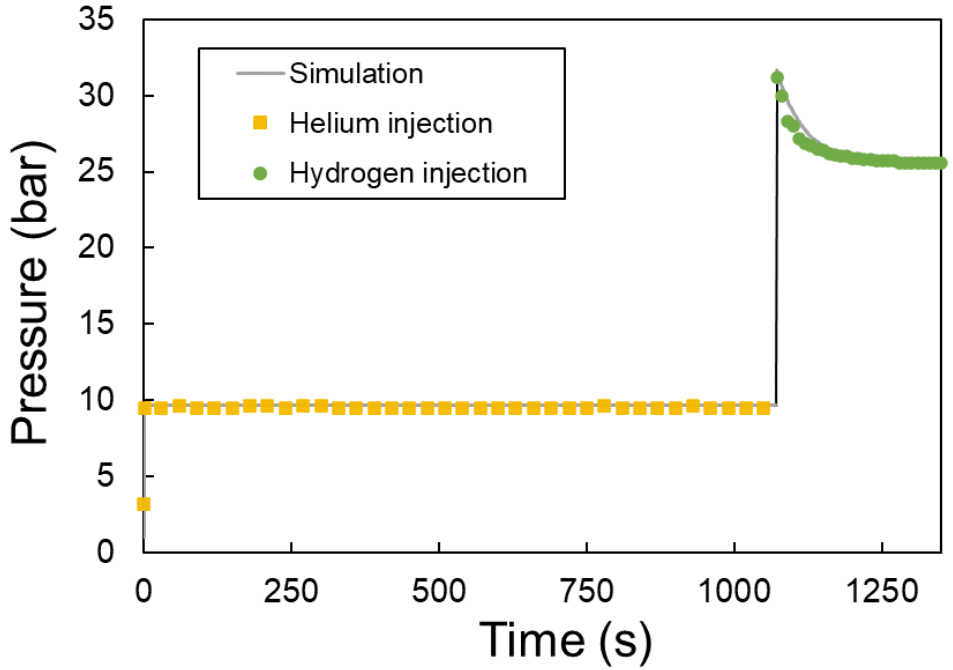

$LaNi_5$ vacuum adsorption cycles

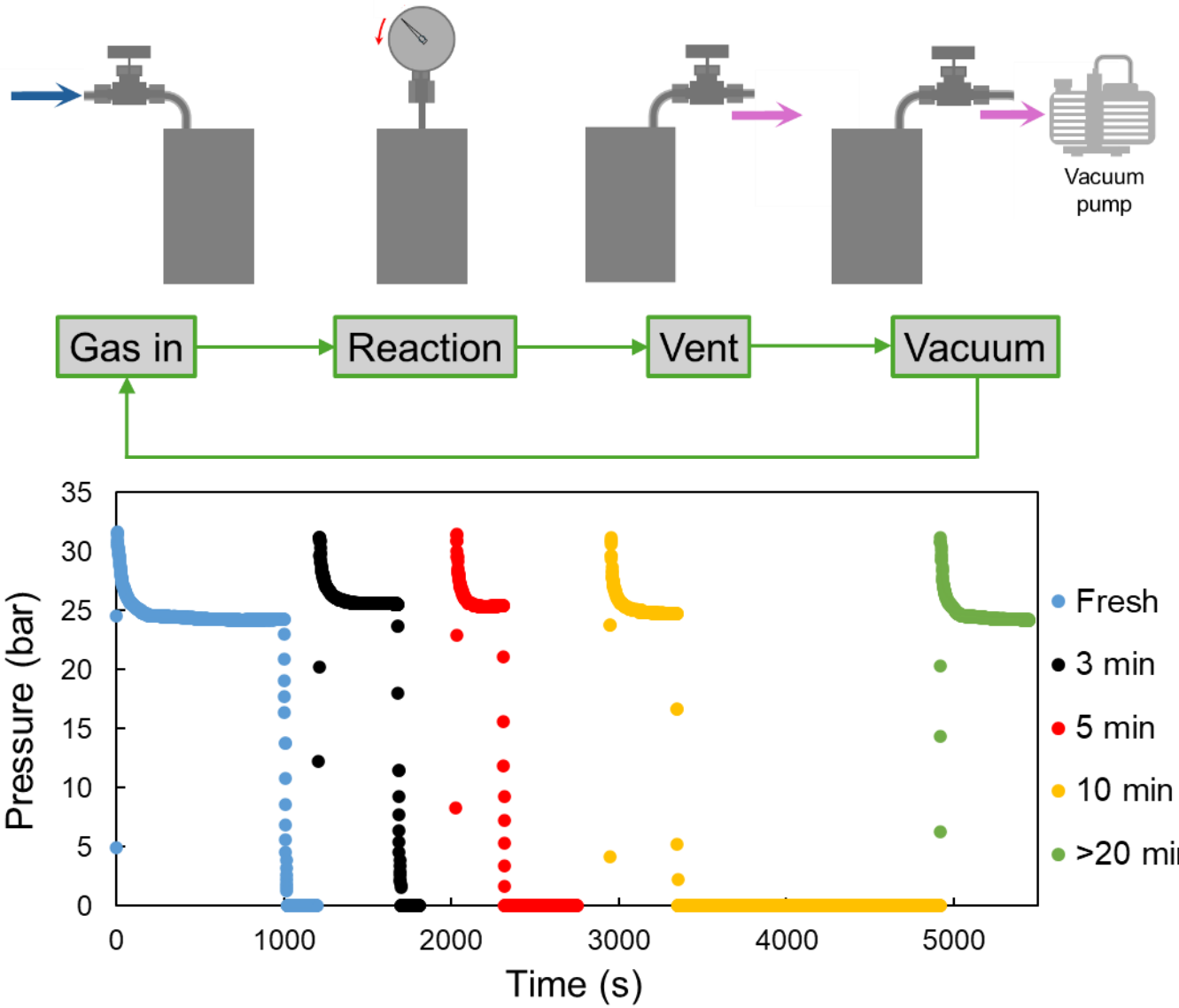

- The hydrogen adsorption and vacuum desorption cycles were performed at 40 °C in the pressure vessel.
- Different vacuum duration was tested to determine the effective working capacity.

Vacuum duration (min)	Adsorption capacity (mol/kg)
Fresh sample	7.01
3	5.48
5	5.86
10	6.34
>20	6.82

VPSA design for He/H_2 separation using $LaNi_5$

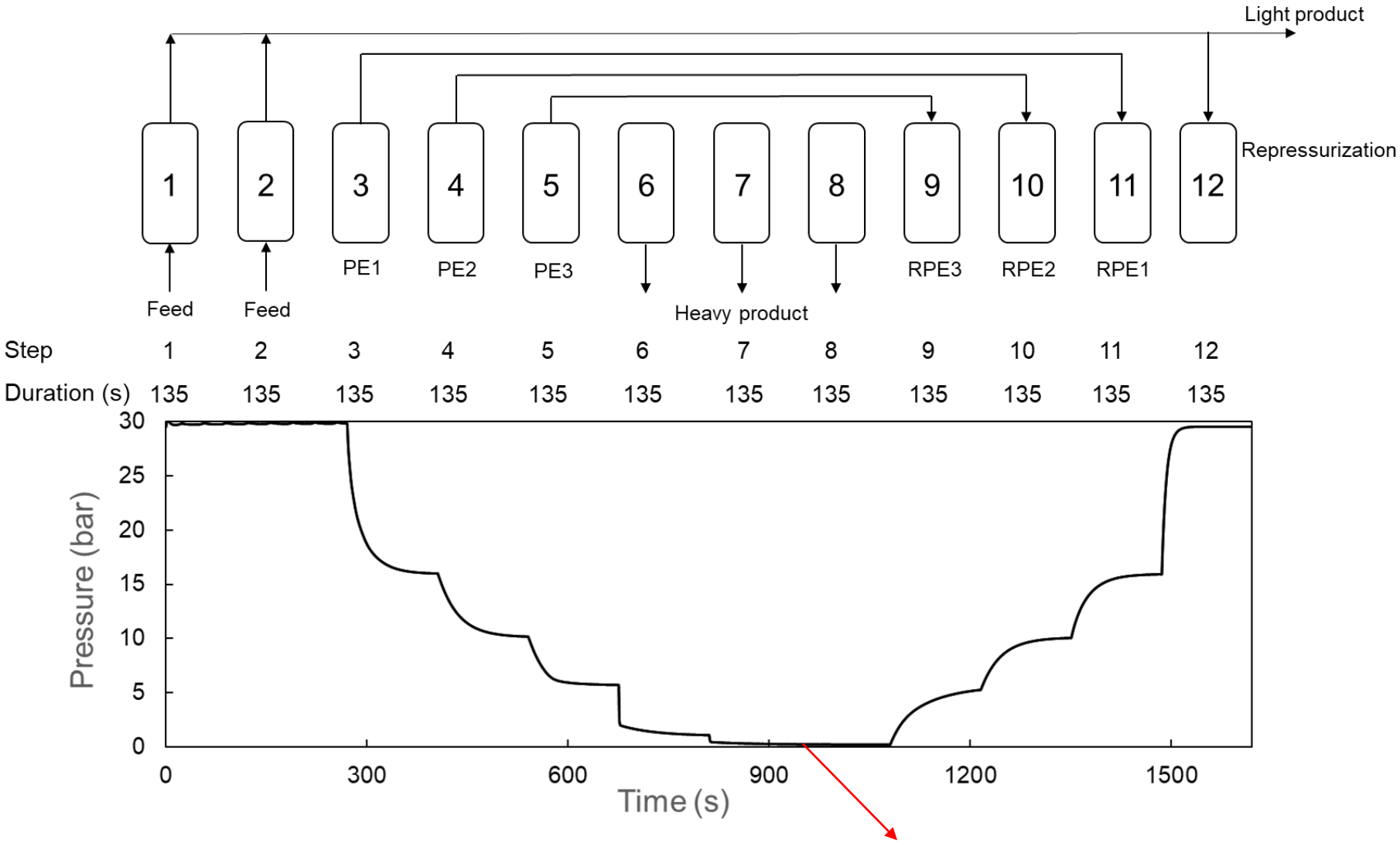

Effect of desorption pressure

(V)PSA column and $LaNi_5$ characteristics used in the simulation (Aspen Adsorption software).

Parameter	Value	Unit
Inlet pressure	30	bar
Column height	0.5	m
Column diameter	0.04	m
Inter-particle voidage	0.33	m^3 void/m^3 bed
Intra-particle voidage	0.248	m^3 void/m^3 bead
Particle radius	2	mm
Bulk solid density of adsorbent	3354.9	kg/m^3
Feed hydrogen concentration	90	%
Temperature	313	K
Flowrate	30	st.L/min

(V)PSA separation performance

Desorption pressure (bar)	Outlet gas	Concentration (%)	Recovery (%)	Energy consumption for vacuum	
				kJ/kmol He	kJ/kmol H_2
0.2	Topstream He	99.52	99.82	3.48E+03	3.90E+02
	Downstream H_2	99.97	99.64		
0.3	Topstream He	99.34	99.68	2.62E+03	2.93E+02
	Downstream H_2	99.92	99.63		
0.4	Topstream He	99.17	99.52	1.81E+03	2.01E+02
	Downstream H_2	99.96	99.57		
1	Topstream He	98.54	98.19	0	0
	Downstream H_2	99.81	99.83		

The energy consumption for the cryogenic separation process is approximately **35 times** that of VPSA separation.

Effect of feed hydrogen concentration

Inlet gas composition		Outlet gas	Concentration (%)	Recovery (%)	Adsorption time/cycle time (s)	Feed flowrate	Mass balance (in/out)		Energy consumption for vacuum = 0.2 bar	
									kJ/kmol He	kJ/kmol H_2
He	0.05	Topstream He	99.82	95.78	135	1.339 mol/min = 30.0 st.L/min	He	100.33	8.10E+03	4.08E+02
H_2	0.95	Downstream H_2	99.80	99.99	1620		H_2	100.00		
He	0.1	Topstream He	99.52	99.82	150		He	99.98	3.48E+03	3.90E+02
H_2	0.9	Downstream H_2	99.98	99.64	1800		H_2	100.30		
He	0.25	Topstream He	99.76	97.96	150		He	100.03	1.00E+03	3.27E+02
H_2	0.75	Downstream H_2	99.33	99.92	1800		H_2	99.99		
He	0.5	Topstream He	99.43	98.56	150		He	100	4.97E+02	4.91E+02
H_2	0.5	Downstream H_2	98.58	99.44	1800		H_2	100		

Case 2: Helium production from natural gas

Background-Economics of the Helium Market

- Up to now, the only commercially viable helium source is helium-containing natural gas (NG).
- In the United States, NG with a helium concentration of higher than 0.3% is considered helium-rich and commercially profitable to be recovered , while in Russian, this value is 0.05%.

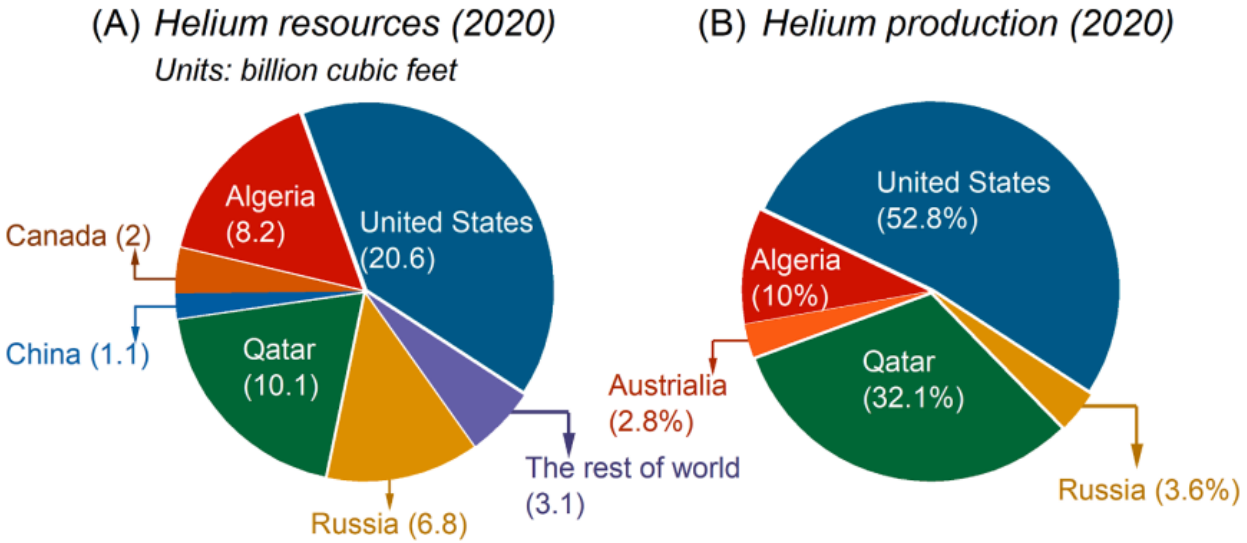

Table 2. Composition of the analyzed gas blend collected from the studied wells in Amadeus Basin. Isotope gas analyses are reported from McInnes et al. (2017).

Well name	Depth (m)	N_2	Ar	He	H_2	CO_2	C_1	C_2	C_{2+}	IC_4/nC_4	IC_5/nC_5	DC	R/R_a	CC
Magee-1	2349	43.61	0.46	6.20	0.03	0.82	39.26	6.10	3.52	0.63	1.11	0.80	–	–
Mt Kitty-1	2144	79.62	–	4.23	5.05	0.33	7.29	2.10	2.85	0.41	8.00	0.71	–	–
Mt Kitty-1	2156	61.04	0.57	8.96	11.4	0.09	13.14	3.53	1.24	0.36	6.50	0.73	0.031[a]	4.4
Mt Kitty-1	2253	99.67	–	0.0	0.0	0.08	0.04	0.02	0.01	0	0	–		
Murphy-1	1647	–	–	–	–	–	1.18	0.01	0.31	0	0	0.79		
Murphy-1	1650	–	–	–	–	–	32.69	2.87	3.90	1.08	0.96	0.83		
Murphy-1	1653	–	–	–	–	–	72.61	3.21	0.99	1.10	0.25	0.94		
Murphy-1	1656	–	–	–	–	–	27.81	3.14	3.61	1.30	0.82	0.81		
Murphy-1	1764	–	–	–	–	–	1.48	0.08	0.16	0	0	0.90		

- Future projection estimates an increase in helium demands of about 6% per year, especially in the semiconductor and medical sectors.

Dai, Z., Deng, J., He, X., Scholes, C. A., Jiang, X., Wang, B., ... & Deng, L. (2021). Helium separation using membrane technology: Recent advances and perspectives. *Separation and Purification Technology*, *274*, 119044.

Double stage VPSA design for helium production from NG

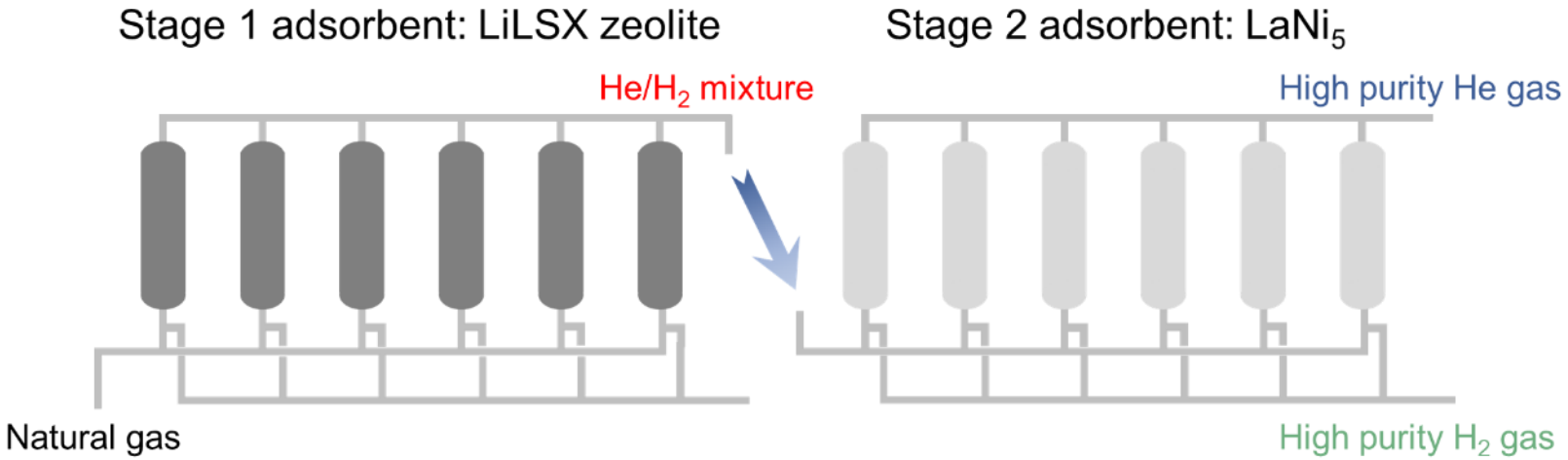

Properties of the adsorption column and running conditions applied in the simulations.

Conditions	Value
Length (m)	0.8
Diameter (m)	0.2
Bed porosity (-)	0.37
Adsorption pressure (bar)	10
Desorption pressure (bar)	0.2
Feed flow rate (mol/min)	20
Temperature (K)	298.15

Table 2
Dual-site Langmuir (DSL) isotherm parameters of different gas components on activated carbon, silica gel and LiLSX zeolite.

	m (mol kg^{-1})	b_0 (bar^{-1})	Q_1 (J mol^{-1})	n (mol kg^{-1})	d_0 (bar^{-1})	Q_2 (J mol^{-1})	Ref.
LiLSX zeolite							
H_2	1.19	8.91E−05	12,433	0.93	5.15E−05	12,378	This work
N_2	1.09	1.68E−05	27,586	1.23	1.64E−05	23,628	This work
CH_4	2.11	5.05E−05	23,357	3.82	2.17E−05	17,574	This work
CO_2	3.04	4.99E−04	31,817	2.60	1.79E−09	33,032	This work
C_2H_6 [b]	0.72	3.18E−04	10,821	2.97	1.18E−05	33,293	This work

[a] Adsorption equilibrium data of C_5H_{12} is assumed for heavy hydrocarbons (C_{4+}) in simulation study.
[b] Adsorption equilibrium data for C_3H_8 and C_{4+} on LiLSX zeolite is assumed to be the same as zeolite5A [35,36,51] in simulations due to experimental limitations and no available data in literature for LiLSX zeolite. This assumption is deemed to be acceptable due to close isotherms of measured gases on both zeolite 5A and LiLSX, and since heavy hydrocarbons are removed prior to reaching the top layer.

Dehdari, L., Burgers, I., Xiao, P., Li, K. G., Singh, R., & Webley, P. A. (2022). Purification of hydrogen from natural gas/hydrogen pipeline mixtures. *Separation and Purification Technology*, *282*, 120094.

Double stage VPSA design for helium production from NG

Gas composition	N_2	C_1	H_2	He	C_2	C_2+	CO_2
Concentration (%)	6E-2	3E-2	50.15	49.76	<1E-5	<1E-5	<1E-5

Stage 1 adsorbent: LiLSX zeolite

$He+H_2$ purity > 99.9%, pressure = 9.9 bar

Stage 2 adsorbent: $LaNi_5$

He purity = 99.25%
recovery = 93.72%

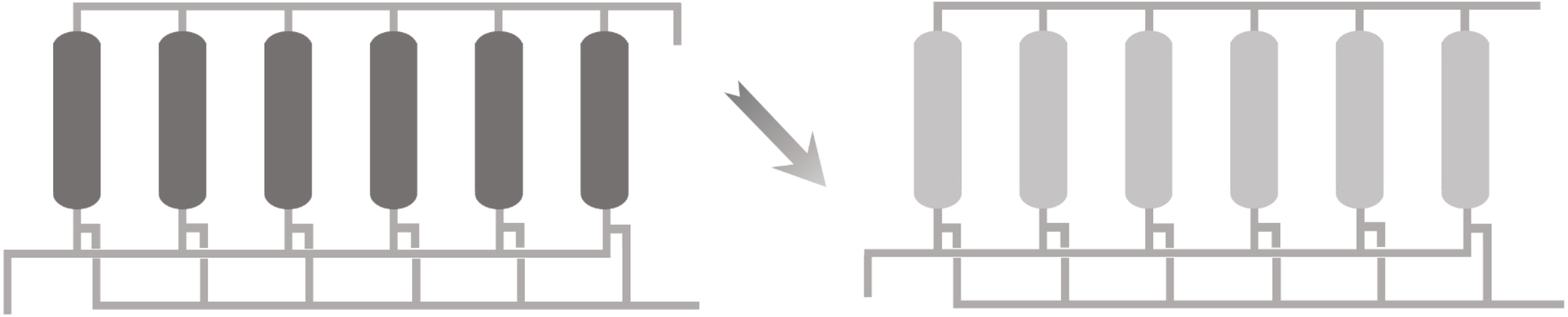

10 bar Natural gas

$He+H_2$ purity > 99.9%, pressure = 9.9 bar

H_2 purity = 99.33%
recovery = 80.2%

Gas composition	N_2	C_1	H_2	He	C_2	C_2+	CO_2
Concentration (%)	61.04	13.14	11.4	8.96	3.53	1.24	0.09

Tech 3 summary

- $LaNi_5$ has selectivity towards hydrogen and can be used for hydrogen and helium separation.
- The experiment results demonstrate that hydrogen can be successfully captured at high pressures and released under vacuum conditions by the alloy $LaNi_5$.
- The designed multiple bed vacuum pressure swing adsorption (VPSA) process has been modeled with Aspen Adsorption simulation tool.
- High purity hydrogen products and helium products (both >98%) can be obtained from the designed VPSA process with high recovery exceeding 95%.

Conclusion and outlook

Conclusion

- Hydrogen selective materials were successfully screened and selected.
- These materials were thoroughly characterized, and their mechanisms were carefully investigated.
- The hydrogen separation processes were designed, simulated, and shown to be both effective and energy-efficient.
- This study highlights the feasibility and effectiveness of PSA technologies in high-purity hydrogen gas separation, supporting the integration of the hydrogen economy into the industry.

Outlook

- The library of hydrogen-selective materials can be further studied to deepen our understanding.
- Additionally, the VPSA design can benefit from further configuration optimization.
- Exploring strategies for larger-scale deployment and scaling up the process will be crucial for future applications.

Acknowledgement

Prof. Paul Webley

Dr. Ali Zavabeti

Dr. Penny Xiao

Dr. Leila Dehdari

A/Prof. Anthony Stickland

Dr. Ranjeet Singh

Dr. Kaifei Chen

Dr. Yalou Guo

Dr. Yuhan Men

Jianing Yang

Jining Guo

Chao Wu

Jia Ming Goh

Zhi Yu

Dingqi Wang

Jianan He

Lei Dong

Xichao Zhang

Yongqiang Wang

Fahimeh Gholampoursaadi

Dr Longbing Qu

Dr Qiuran Yang

Dr Joshua Butson

Dr Qining Fan

Thanks for your attention!

Enabling the decarbonisation of Australia's energy networks

futurefuelscrc

futurefuelscrc.com

Future Fuels CRC is supported through the Australian Government's Cooperative Research Centres Program. We gratefully acknowledge the cash and in-kind support from all our research, government and industry participants.

Australian Government
Department of Industry, Science and Resources

AusIndustry
Cooperative Research Centres Program